Seismicity Report on the
DIXIE VALLEY PROSPECT
Churchill County, Nevada

ABSTRACT

For twenty days in October and November of 1976, 200
square kilometers north of the Dixie Hot Springs in Central
Nevada were surveyed for microearthquakes by use of a high
gain (1-6M), high frequency (5-30Hz passband) seismic
network. 216 events were detected in the immediate area.
Fault-plane solutions indicate that the faulting in this
area is an extrapolation of the tectonic style found in the
major fault zones to the south. Conclusions are that fault
intersections occur on the prospect, and, while their
seismicity rate is not exceptional, the prospect is
seismologically favorable for the occurrence of a geothermal
reservoir. Confirmation of a heat source and a favorable
hydrologic regime by electrical resistivity surveys is
recommended. Caution should be observed because of
recognized seismic risk in this area.

TABLE OF CONTENTS

FIGURES AND TABLES

INTRODUCTION

A microearthquake survey to aid in the evaluation of the geothermal potential of the Dixie Valley prospect, Churchill County, Nevada, was conducted by MicroGeophysics (MGC) for twenty days in October, 1976. The prospect is near the Humbolt Salt Marsh and the Dixie Hot Springs (see the location and index map, Figure 1) in west central Nevada.

A high gain (1-6M at 20hz) high frequency (5-30 hz passband) seismic network (see instrument appendix) of 7 to 10 stations was deployed to survey the surrounding 200 km^2 for discrete, natural seismic events (microearthquakes) and thereby map tectonically active structures. The existence of recurrent, active tectonic processes is thought to be a necessary, but not sufficient, condition for the occurrence of commercial geothermal energy (Lange and Westphal, 1969; Ward and Bjornson, 1971; Ward and Jacob, 1971; Hamilton and Muffler, 1972; Ward, 1972). Although debate concerning acceptable geologic models for a geothermal system is continuing, an active tectonic system and the associated fracture porosity and permeability is an attractive target for geothermal exploration efforts. However, a seismically active system does not guarantee a heat source or the sufficient ground water supply necessary for a geothermal occurrence.

Sections of this report and their contents are listed below. The next section is a brief geological summary which includes a summary of the historical seismicity. Next is the operations summary which includes the survey parameters such as the magnitude detection threshold, the error prediction analysis, the velocity model, and the individual station parameters. The section on results contains the factual data obtained from the survey. Interpretation of these results is followed by the final sections which are the summary conclusions and recommendations of this report.

PROSPECT

39°45'N
118°00'W

5   0   5   10

KILOMETERS

NEVADA

• RENO   ☐
          PROSPECT

40°

N

0   200
    KM

36°

116°
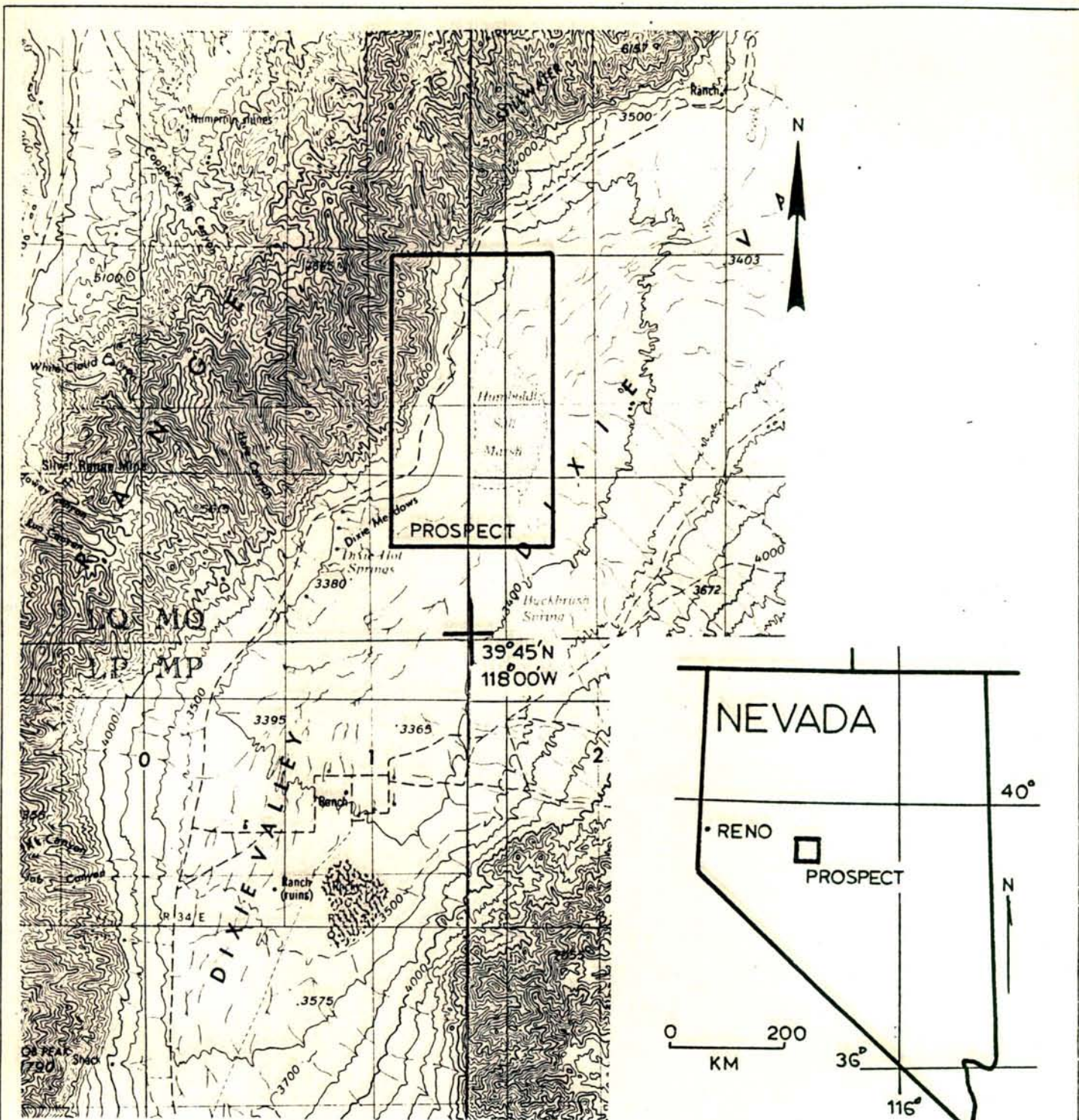
DIXIE VALLEY PROSPECT
CHURCHILL COUNTY, NEVADA

TITLE:	LOCATION AND INDEX MAP	
SCALE: *N/A*	APPROVED BY: *JRB*	DRAWN BY *PB*
DATE: DEC 13, 1975		REVISED *N/A*
Micro Geophysics		Figure 1

GEOLOGICAL AND GEOPHYSICAL BACKGROUND

The Dixie Valley prospect lies in the Basin and Range province. The area is characterized by north to north-northeast trending ranges separated by narrow valleys. Dixie Valley lies between the Stillwater mountains on the west and the Clan Alpine mountains on the east.

The following is a brief summary of the lithology of the major rock units in the prospect area followed by a brief description of the tectonics in the area. A schematic of the geology is shown in Figure 2.

Triassic metasediments and Upper Jurassic and Tertiary intrusives, volcanics and metavolcanics are exposed in the prospect area. Upper Triassic slate and phyllite is found at the southern end of the survey area. The Upper Jurassic Humboldt Gabbroic Complex is exposed in the eastern portion of the Stillwater range. This unit consists of shallowly emplaced gabbro and diorite that apparently broke the sur- face occasionally during intrusion forming an extrusive sequence of basalt flows, tuffs and breccias (Meister, 1967). Scattered early Tertiary plutons and diverse volcanics are also found in the Stillwaters. Capping the range and covering much of this area are 1800-4000' of Miocene vol- canics including tuffs, breccias and a wide compositional range of flows. Dixie Valley is covered by unconsolidated lake and stream sediments of Plio-Pleisocene to recent age.

118°15' 118°00' 117°45'

40°00'

PROSPECT

DIXIE VALLEY

39°45'

FAULT

N

39°30'

5 KM

	Tertiary	basalt and andesite
		non-marine sediments & tuffs
		tuffs & flows of rhyolite, dacite
		undiff. pre-lahontan sediments & volcanics
		granitic intrusives
		latite, rhyolite, basalt
		basalt flows, tuffs, & breccias
		gabbroic & dioritic intrusives
Mesozoic		metavolcanic tuffs, breccias & flows
		limestone
		slate & phyllite

(AFTER MEISTER, 1967)

TITLE: GEOLOGIC MAP		
SCALE: N/A	APPROVED BY: JRB	DRAWN BY PB
DATE: DEC 14, 1975		REVISED N/A
Micro Geophysics		DRAWING NUMBER Figure 2

(5)

These include fan detritus, stream channel deposits and lacustrine sediments of primarily silt and clay.

Several major thrust faults are evident in the Stillwater Range. Triassic slates are underlain by a brecciated fault zone. In the north the slate rests disconcordantly on quartzite which overrides Jurassic metavolcanics which in turn overrides an undated limestone. Thus, to the north an imbricate-thrust zone is present. Elsewhere, gabbro of the Humboldt Gabbroic Complex overrides Triassic slate. It has been suggested that the shallow intrusion of the Humboldt Complex caused the motion of the thrust sheet. The suggested motion implies a late Jurassic age for the thrusting.

Cenezoic normal faulting has uplifted the Stillwater Range as a horst of narrow, north-trending blocks typical of Basin and Range structure. The attitude of basalt flows in the blocks evidences tilting of up to 12°. In some cases interior normal faults extend to the range margin, becoming part of the boundary fault. Often a series of step faults comprise the boundary fault with as many as four normal faults contributing to the structural relief between the range and valley (Herring, 1967).

The Dixie Valley fault has been active in historic time (Figure 2). Movement on this fault occurred at the time of the December 16, 1954 earthquake (Romney, 1957).

Displacement observed on surface faults was predominantly dip-slip in the Dixie Valley while it became diagonal-slip and strike-slip in the southern part of the fault system (Slemmings, 1957).

The historical seismicity and its relation to the geology will be discussed next. Dixie Valley is in the Nevada Seismic Zone and contains the northern end of a linear zone of concentrated seismic activity extending north from the Fairview Range. The source of this activity is the boundary fault between the Fairview Range and the Bell Flat grabben, the continuation of the boundary fault to the north, and the Dixie Valley Fault (Westphal and Lange, 1967). Movements on these faults were the source of energy for the 1954 earthquakes of magnitudes exceeding 6.

Figure 3 is a plot of epicenters showing the seismic activity for two years, 1970 and 1971. The north-south trending pattern labeled A is the Fairview Peak-Dixie Valley seismic zone. Historically no earthquakes
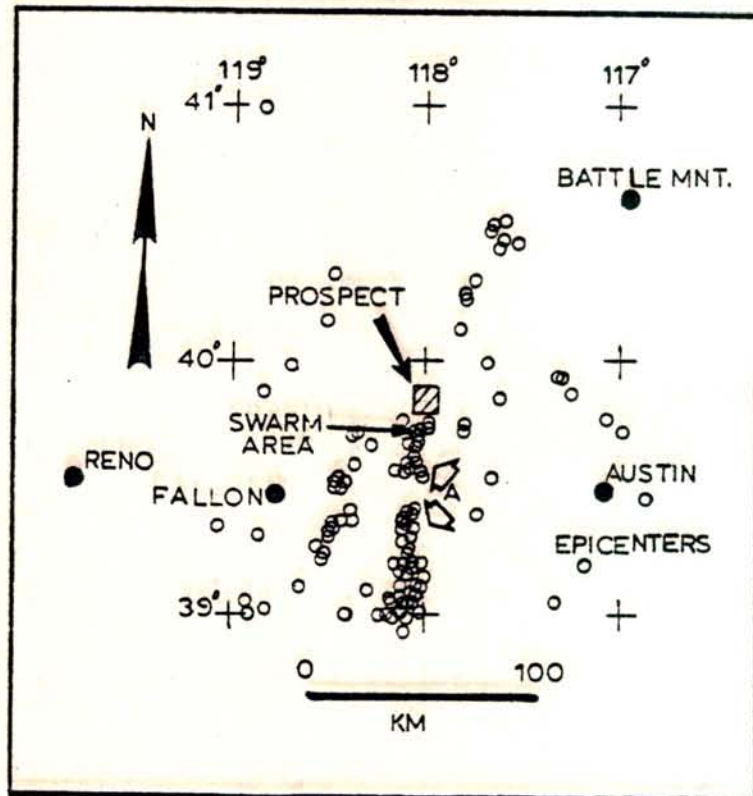

Figure 3. Historical Seismicity
(after Nevada Bureau of Mines)

have occurred in the prospect area. The historical seismic activity is truncated just south of the prospect near Dixie Hot Springs, with a very active swarm center near the Dixie Hot Springs (Figure 3).

According to Gumper and Scholz (1971), the movement on the Dixie Valley fault is dip slip with minimal strike-slip. From observing the vertical displacement of the surface faulting, they excluded the possibility of a significant horizontal component. However, it appears that more than a single fault plane is needed as a mechanism to explain the observed seismicity of this fault system. At the southern extreme of the Fairview Peak fault, microearthquake hypocenters are concentrated at 10-15 km depth and are near the end of the surface faulting associated with the 1954 earthquakes (Stauder and Ryal, 1967). The hypocenters define two planar zones, one striking N 10° W and dipping 62° E, the other N 50° E, 50° SE. The former conforms with the trend of the whole Dixie Valley-Fairview Peak fault system. Surface faulting is terminated at the intersection of the two planes suggesting that the latter plane is a cross fault truncating the main system.

More recent microearthquake work in the Fairview Peak area has led to a more detailed model of the fault mechanism (Douglas and Ryall, 1972; Ryall and Mallone, 1971). They propose a zig-zag fault system consisting of northeast

trending tensional cracks and
north-northwest trending
compressional fractures
(Figure 4). Motion on the
Dixie Valley fault yields a
fairly well-determined solu-
tion of right lateral oblique
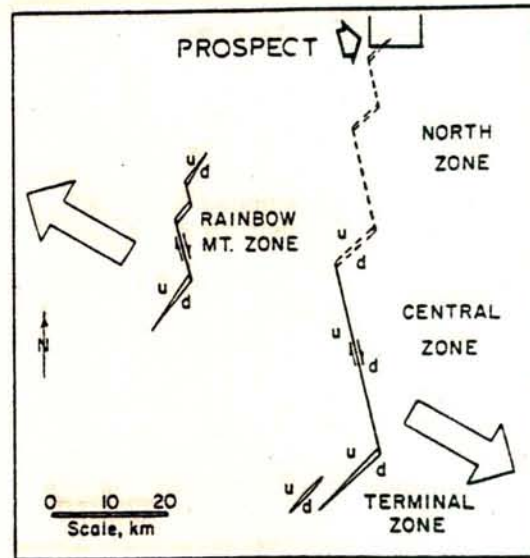slip on a northeast trending
fault plane.

Figure 4. Fault Model
(after Ryall and Malone,
1971)

OPERATION SUMMARY

Ten seismic stations were used in the course of this
survey. The technical description of the instruments is
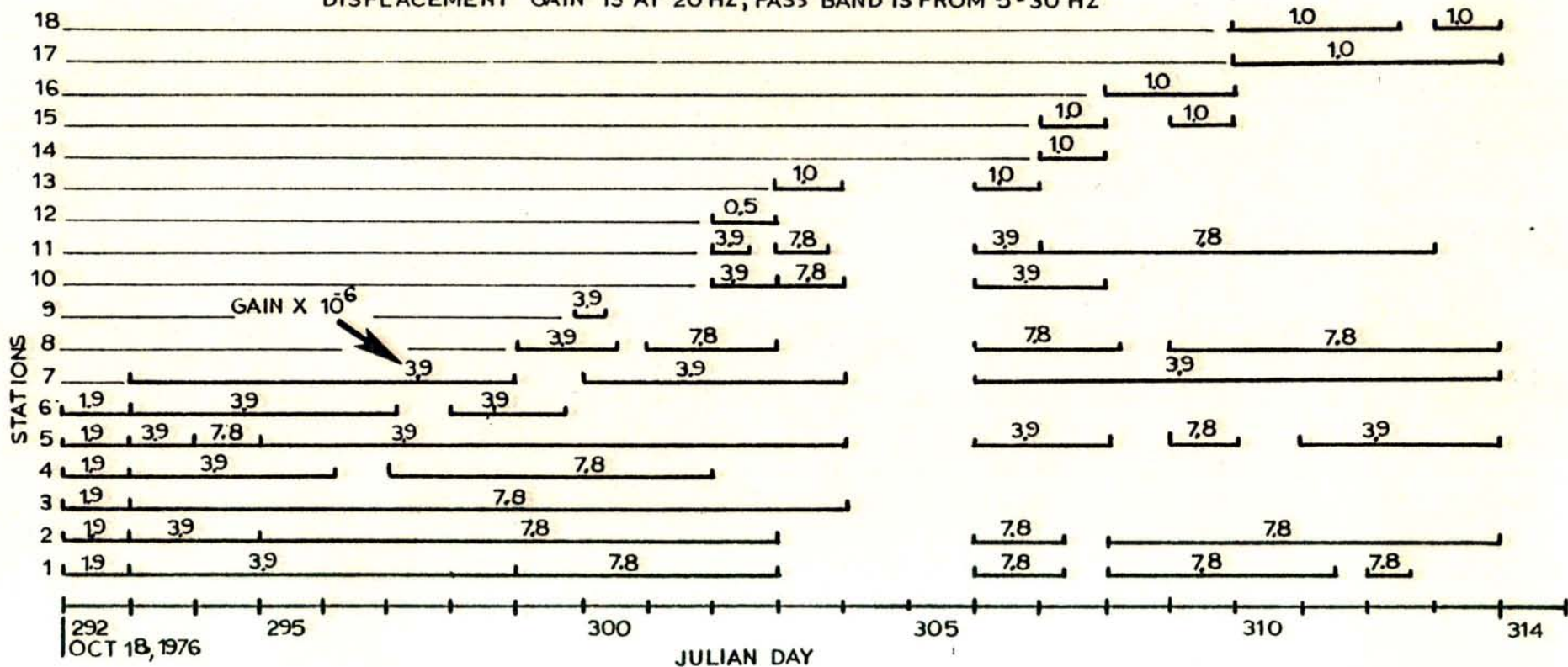included in an appendix to this report.

Most stations were located on hard rock outcrops, ex-
cept where array-geometry considerations dictated otherwise.
Hardrock outcrop stations are superior to alluvial stations
in both signal quality and the amount of ambient background
noise. The increase in ambient background noise from an
alluvial station to a nearby hard-rock station can often
be 20 db. Therefore the signal-to-noise ratio of a network
is improved if the majority of stations are placed on hard
rock. Stations not placed on hard rock included stations 12,
13, 14, 15, 16, 17, and 18. At any one time during the
survey no more than two of these stations were occupied.

Station locations were changed to maximize instrument
gain and azimuthal coverage of the project area. All
stations were operated at the gain limit allowed by the
ambient background noise level. Table 1 is a detailed
operational summary for the twenty day period of this
survey. Coordinates of the seismograph stations are
listed in Table 2 and displayed on Figure 5.

A detection threshold map (Figure 6) shows that the

TABLE 1   OPERATION SCHEDULE

DISPLACEMENT GAIN IS AT 20 HZ, PASS BAND IS FROM 5 - 30 HZ

STATIONS (vertical axis, 1–18)

GAIN X 10^{-6}

Values shown along station lines:

- 18: 1.0 ... 1.0
- 17: 1.0
- 16: 1.0
- 15: 1.0 ... 1.0
- 14: 1.0
- 13: 1.0 ... 1.0
- 12: 0.5
- 11: 3.9 ... 7.8 ... 3.9 ... 7.8
- 10: 3.9 ... 7.8 ... 3.9
- 9: 3.9
- 8: 3.9 ... 7.8 ... 7.8 ... 7.8
- 7: 3.9 ... 3.9 ... 3.9
- 6: 1.9 ... 3.9 ... 3.9
- 5: 1.9 ... 3.9 ... 7.8 ... 3.9 ... 3.9 ... 7.8 ... 3.9
- 4: 1.9 ... 3.9 ... 7.8
- 3: 1.9 ... 7.8
- 2: 1.9 ... 3.9 ... 7.8 ... 7.8 ... 7.8
- 1: 1.9 ... 3.9 ... 7.8 ... 7.8 ... 7.8 ... 7.8

292 OCT 18, 1976   295   300   305   310   314

JULIAN DAY

Table 2.

DIXIE VALLEY STATION COORDINATES

Station	X (km)	Y (km)	Z (km)
1	13.2	32.1	1.16
2	11.1	35.7	1.41
3	19.8	45.0	1.24
4	18.8	43.5	1.33
5	19.8	39.1	1.15
6	17.0	36.6	1.21
7	21.1	36.2	1.14
8	16.3	37.3	1.27
9	17.5	43.8	1.58
10	15.3	45.4	2.15
11	16.7	40.7	2.05
12	21.4	43.2	1.06
13	21.8	44.8	1.06
14	20.8	42.1	1.06
15	20.6	44.0	1.12
16	21.1	41.1	1.04
17	22.8	43.3	1.03
18	20.6	40.3	1.03

The origin is located at latitude 39°30' N, longitude 118°15'W. Z is the station altitude above sea level. Positive X and Y are east and north respectively. The accuracy of the coordinates are ± 0.10 km in X and Y and ± 0.02 km in Z.
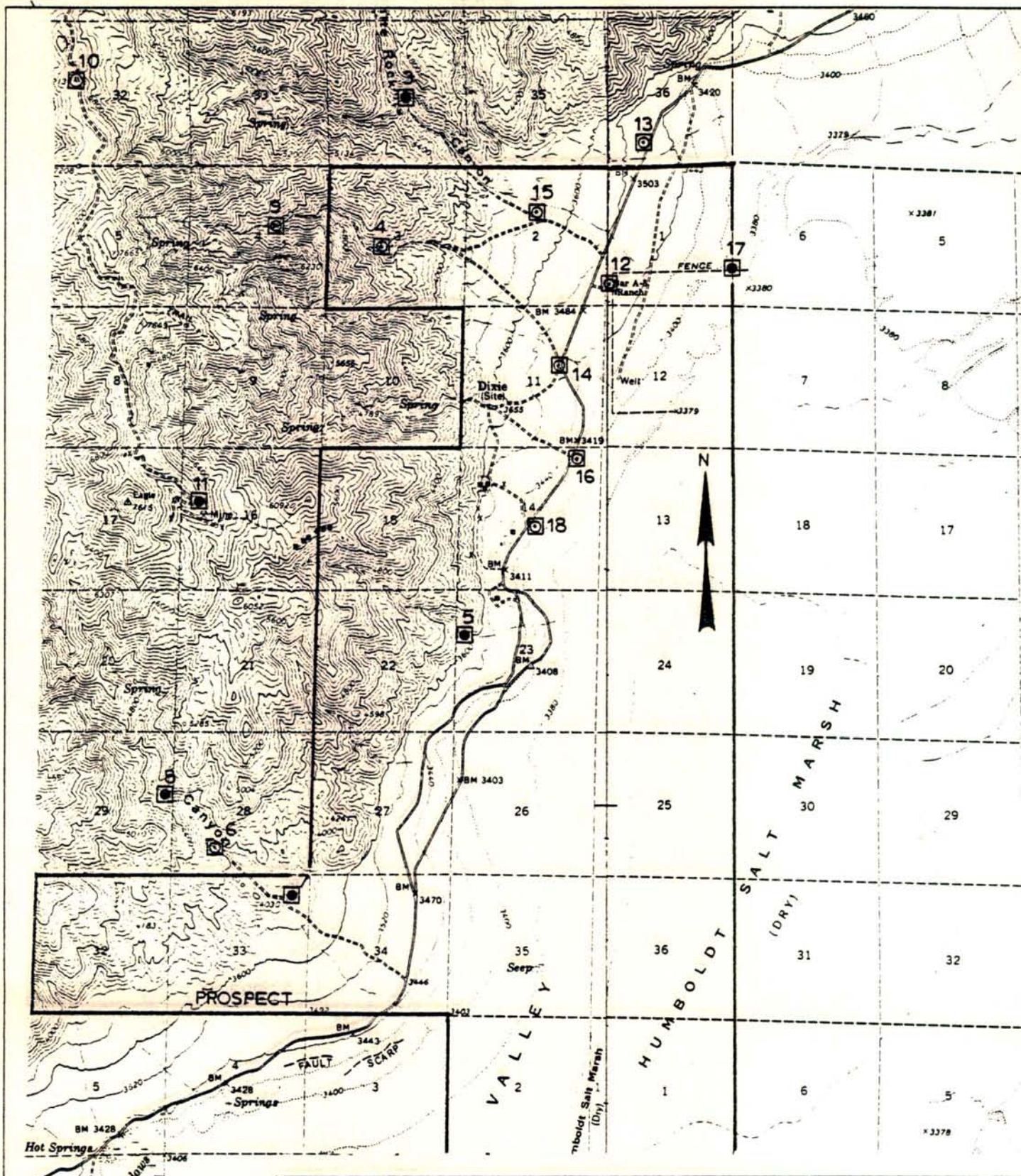
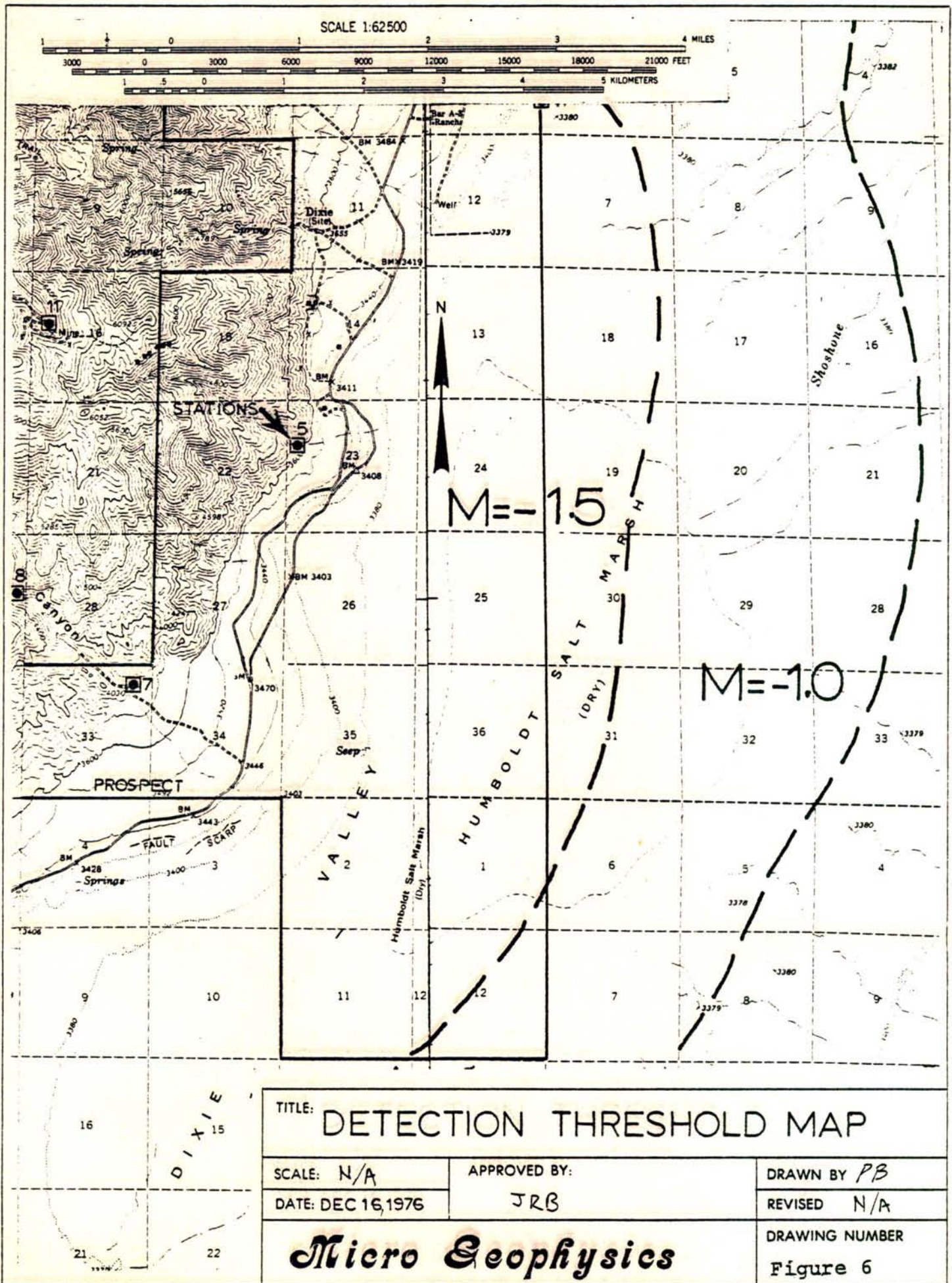| TITLE: STATION LOCATION MAP		
SCALE: N/A	APPROVED BY: JRB	DRAWN BY PB
DATE: DEC 16, 1976		REVISED N/A
Micro Geophysics		DRAWING NUMBER Figure 5

prospect area was surveyed for microearthquakes of magnitude
-1.5 and larger. The line labeled "Mag.=-1" on Figure 6
is the surface projection of the volume within which a
-1.0 magnitude earthquake would give at least a 2mm peak-to-
peak displacement on at least one of the network stations.
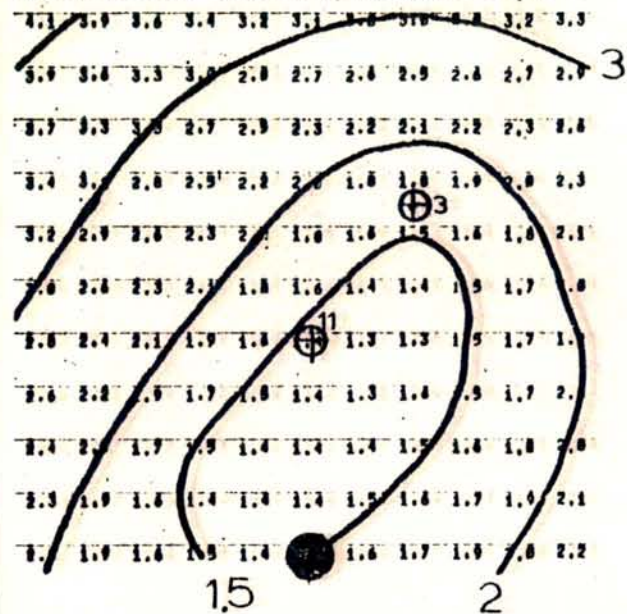The analysis assumes normal attenuation as described by Brune
and Allen (1967).

To further evaluate the seismic network, the technique of
error prediction analysis (Peters and Crosson, 1972) was used
to contour the expected precision of two of the station con-
figurations. This technique requires an estimate of the un-
certainties of the arrival times, velocity, and origin-time.
Figures 7 and 8 show the estimates used and contours of the
standard deviation of location parameters produced by the
listed uncertainties. Thus the uncertainty of locations is
generally ± 1.0 km in plan and ± 2.0 km in depth throughout
the area of interest. The depth error increases rapidly away
from the stations.

The velocity model is derived from previous work and from
recordings of local events. Events were regarded as seismic
in origin if they appeared on two or more stations with time
difference corresponding to expected seismic velocities or
if they had a signature similar to other larger events which
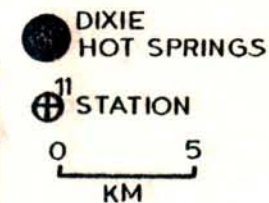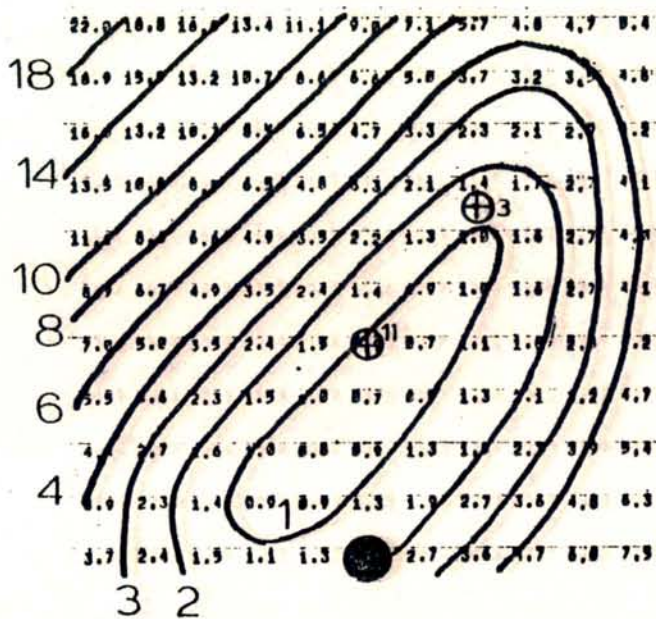could be traced across the network. Events were considered

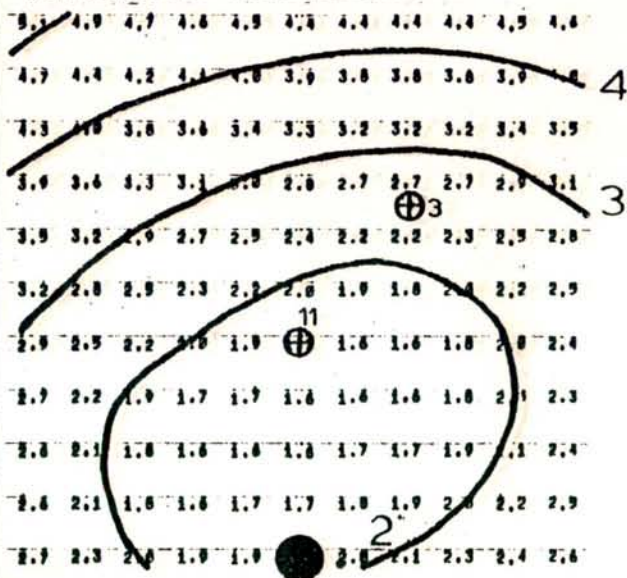SCALE 1:62500

STATIONS

M=-15

M=-10

TITLE:	DETECTION THRESHOLD MAP	
SCALE: N/A	APPROVED BY: JRB	DRAWN BY PB
DATE: DEC 16, 1976		REVISED N/A
Micro Geophysics		DRAWING NUMBER Figure 6

PREDICTED UNCERTAINTIES FOR X

PREDICTED UNCERTAINTIES FOR Z

● DIXIE HOT SPRINGS

⊕¹¹ STATION

0   5
    KM

PREDICTED UNCERTAINTIES FOR Y

DIXIE VALLEY PROSPECT

AREA: $6 \leq X \leq 26$ KM
       $32 \leq Y \leq 52$ KM

CONTOUR INTERVAL:
    KM

HYPOCENTRAL DEPTH:
    4 KM

VELOCITY MODEL:
    HALF SPACE 4.5 KM/SEC

UNCERTAINTIES
    TIME: + 30ms
    VEL: 0.1 KM/sEC
    ORIGIN
    TIME: 0.300 SEC

TITLE: PREDICTED UNCERTAINTIES, AREA 1		
SCALE: N/A	APPROVED BY: JRB	DRAWN BY PB
DATE: DEC 16, 1976		REVISED N/A
Micro Geophysics		DRAWING NUMBER Figure 7

(17)

PREDICTED UNCERTAINTIES IN X

PREDICTED UNCERTAINTIES IN Z

● DIXIE
HOT SPRIGS

⊕ STATION

N

0   5
|——————|
KM
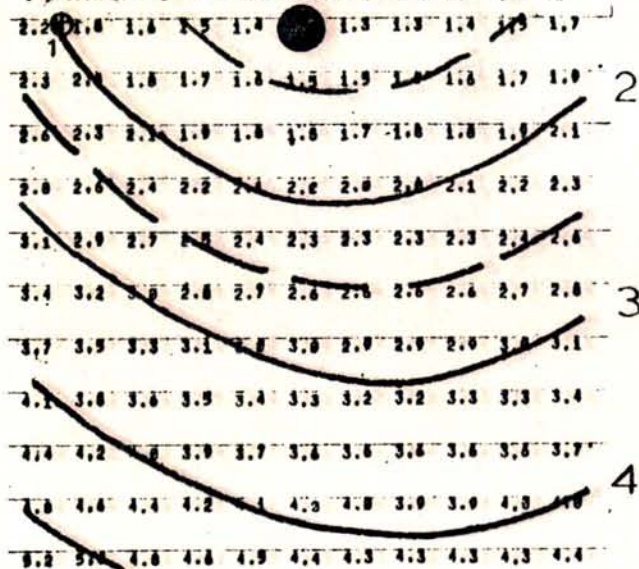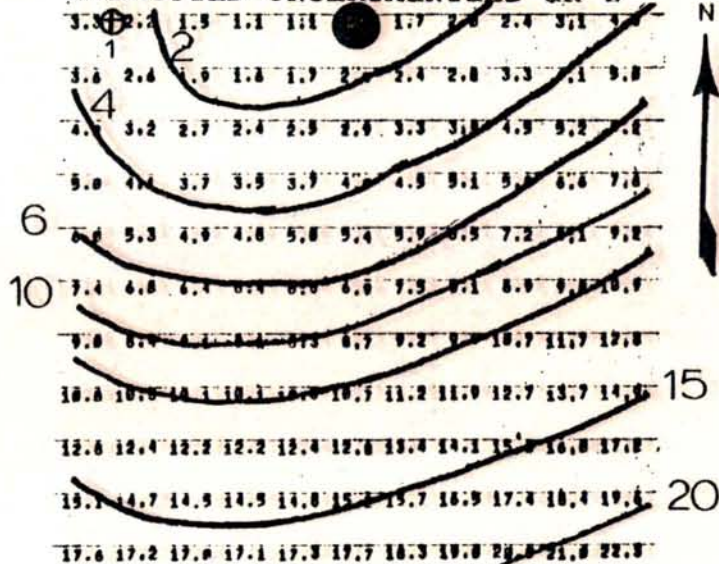
PREDICTED UNCERTAINTIES IN Y

DIXIE VALLEY PROSPECT

AREA: $6 \leq X \leq 26$ KM
       $12 \leq Y \leq 32$ KM

CONTOUR INTERVAL:
       KM

HYPOCENTRAL DEPTH
4 KM

VELOCITY MODEL:
       HALF SPACE 4.5 KM/SEC

UNCERTAINTIES
       TIME: +30 ms
       VEL: 0.1 KM/SEC
       ORIGIN
       TIME: 0.300 SEC

TITLE: PREDICTED UNCERTAINTIES, AREA 2		
SCALE: N/A	APPROVED BY: JRB	DRAWN BY PB
DATE: DEC 16,1976		REVISED N/A
Micro Geophysics		DRAWING NUMBER Figure 8

(18)

local if they had an S-P time of less than three seconds. Regional events and teleseisms were identified by signature and by S-P time. Regional events and teleseisms were considered outside the scope of this survey and therefore, no further analysis was performed on them.

Local events, timed on four or more stations, were located using a generalized-inverse computer program. This program, given a velocity model, least-square fits the calculated travel times to the observed arrival times. Events were read to ± 0.01 seconds for P arrivals and ± 0.1 seconds for S-p times. Amplitudes, peak to peak, were read to the nearest millimeter and the direction of the first motion when distinguishable, was noted.

The most critical parameter in the location procedure is the selection of an appropriate velocity model. The first step in this analysis was to run the observations through the location program assuming a constant velocity model, where $V_c = 4.0$ Km/sec. Examination of statistical errors from this fitting procedure gives the interpreter a feel for the consistency of the data and general location of the local seismicity.

A general upper crustal velocity model for the Dixie Valley prospect has been investigated by several authors (Meister, 1967; Eaton, 1963; Hill and Pakiser, 1967). A composite velocity model is shown in Figure 9. Also shown in

Figure 9 is a linear-increase-of-velocity-with-depth model which approximates the composite model $V=V_O+k_z'$:

$$\text{where } V_O=2.5 \text{ km/sec.}$$
$$k = 0.60\text{km/sec/ km}$$

This linear velocity model produced good statistical fits and consistent locations for events recorded on six or more stations. Table 3 (on Figure 9) lists the velocity model comparisons at various depths.
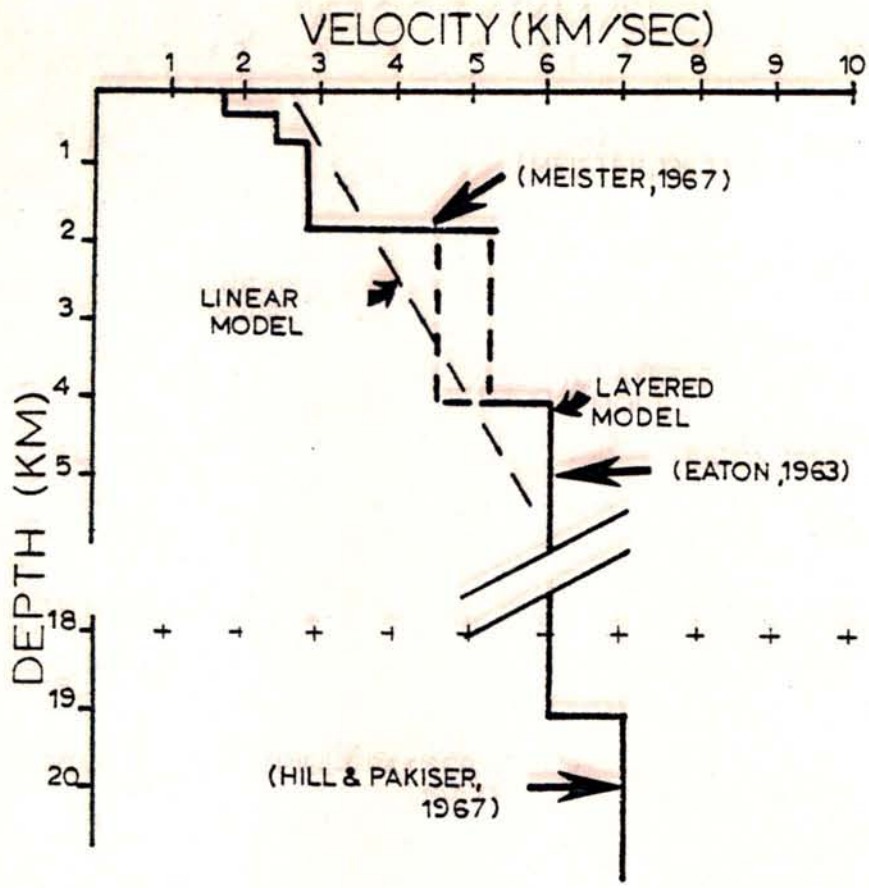
VELOCITY (KM/SEC)

VELOCITY (KM/SEC)

1 2 3 4 5 6 7 8 9 10

DEPTH (KM)

(MEISTER, 1967)

LINEAR MODEL

LAYERED MODEL

(EATON, 1963)

(HILL & PAKISER, 1967)

TABLE 3   VELOCITY MODEL

| DEPTH TO TOP OF LAYER (KM)	0.0	2.0	4.0	19.0
LAYERED MODEL VELOCITY IN LAYER (KM/SEC)	1.75-2.9	4.5-5.3	6.0	7.0
LINEAR MODEL (KM/SEC)	2.5	3.7	4.9	-

OBSERVATIONS

Epicenter Locations

Two hundred and sixteen local seismic events were detected during this survey. Of these, 44 were located. The epicenter map on Figure 10 indicates most of the epicenters occurred just south of the hot springs. The 172 events not located were assigned a location by use of the S-P time and signature similarity to well placed events. Almost all of these events occur in the area south of the hot springs. Of the events that were detected within 2 km of the prospect, 90% were located. Therefore no significant seismic information with respect to the prospect area has been omitted.

The hypocenter map reproduced at a scale of 1:62500 is in the cover leaf of this report. All the located events are shown with time and depth. A listing of all located events is found in the appendix.
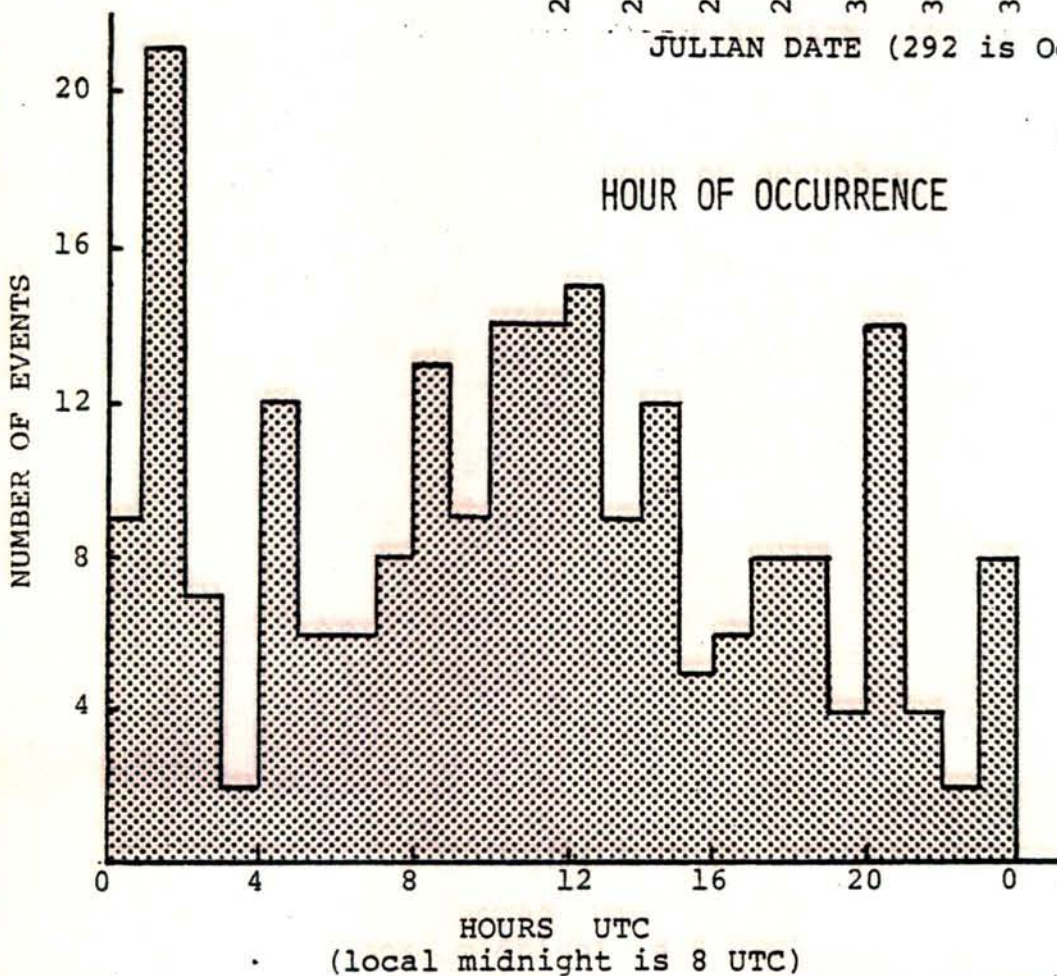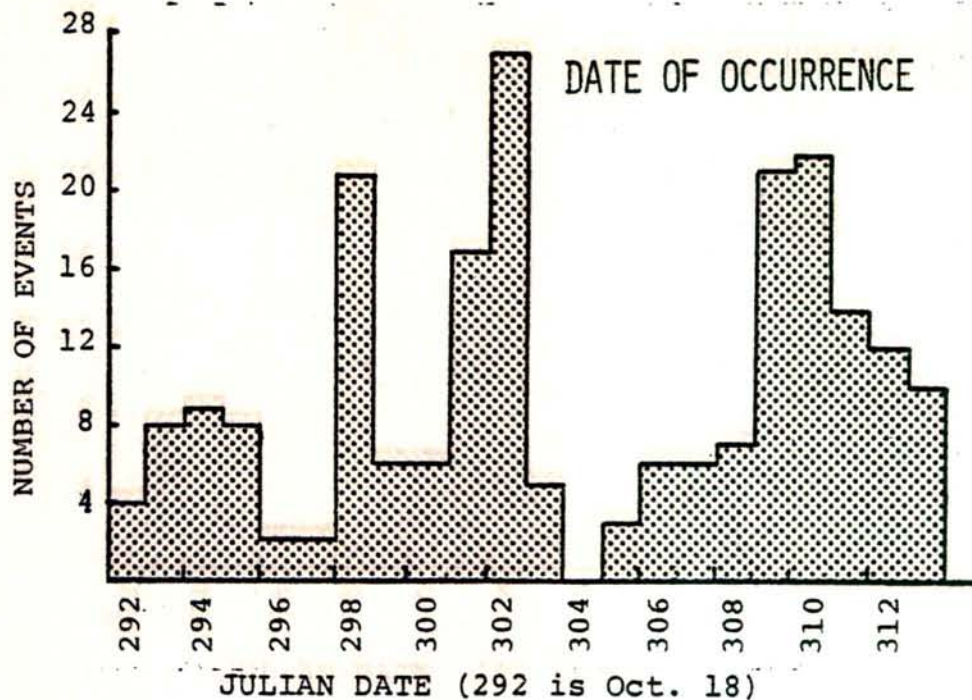
Time of Occurrence

The number of events-by-date (Figure 11) shows an average of above 11 events occurred per day, with increases of activity on days 298, 302 and 309.

The number-of-events-by-hour-of-occurrence curve (Figure 11) can indicate if the seismicity recorded is man made (by having

STATION

STILLWATER RANGE

EPICENTER

DIXIE VA.

N

DIXIE HOT SPRINGS

0   5
KM
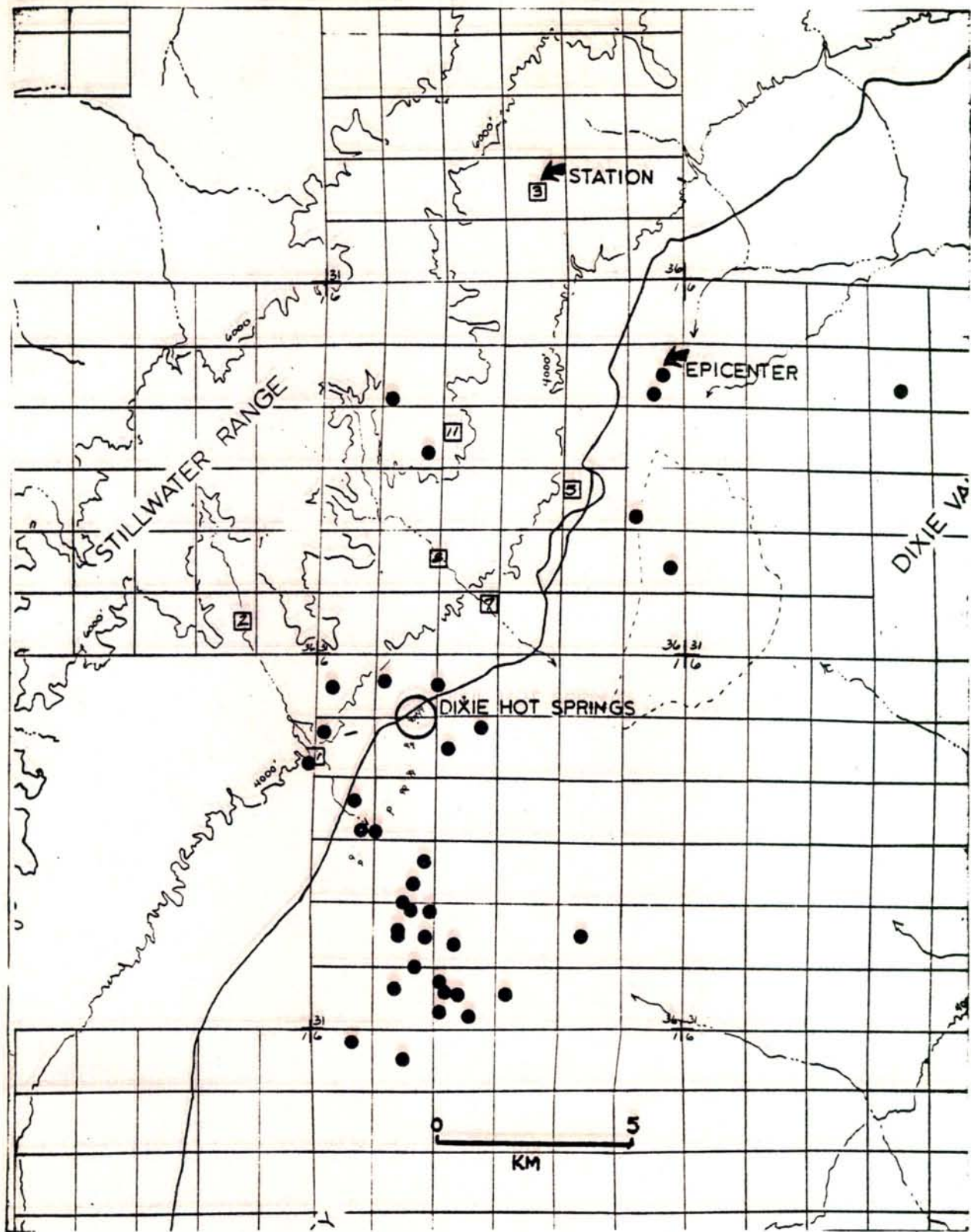
TITLE:		EPICENTER MAP		
SCALE: N/A		APPROVED BY: JRB		DRAWN BY PB
DATE: DEC 18, 1976				REVISED N/A
Micro Geophysics				DRAWING NUMBER Figure 10

DATE OF OCCURRENCE

NUMBER OF EVENTS

JULIAN DATE (292 is Oct. 18)

HOUR OF OCCURRENCE

NUMBER OF EVENTS

HOURS UTC
(local midnight is 8 UTC)

TITLE: OCCURRENCE STATISTICS		
SCALE: N/A	APPROVED BY: PLB	DRAWN BY JRB
DATE: DEC. 14		REVISED N/A
Micro Geophysics		DRAWING NUMBER Figure 11

(24)

obvious peaks between 8 a.m. and 5 p.m. local time (1600 UTC

and 0100 UTC), or if the afternoon cultural and meteorological

noise is covering some events (by having an obvious low from

2 p.m. to 7 p.m. local time, 2200 UTC to 0300 UTC).

The graph of hour of occurrence shows no pattern indi-

cating that either local mining activity (explosives) or

meteorological causes affected the recording of the local

microearthquakes.

Because nearly all events were well-recorded on station

#2, the amplitudes of the p-wave on station 2 was used to

calculate the magnitude. Using the station 2 amplitudes and

the distance from Station 2 to the hypocenter a calculation

of the magnitude can be made using curves developed by
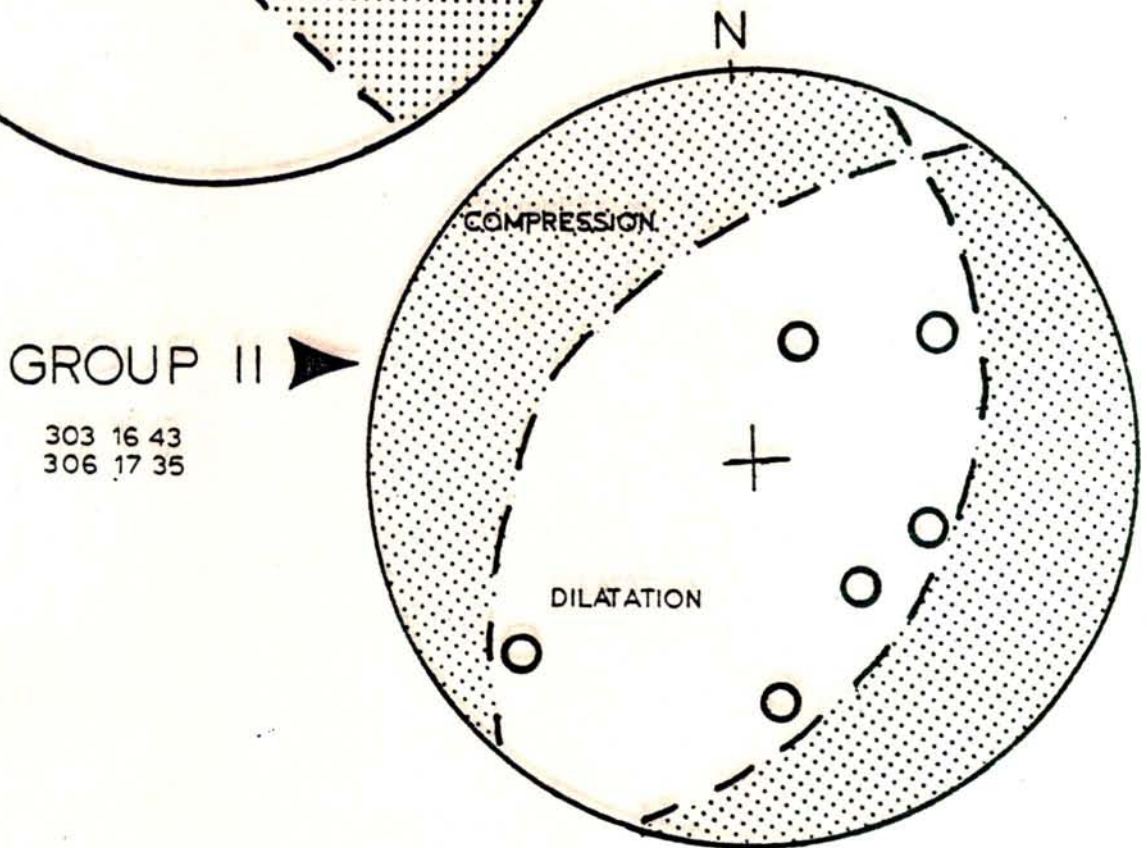
Brune and Allen (1969).

The magnitudes calculated were then used to construct

the recurrence curve of Figure 12. A reference line with a

slope of -0.9 is shown on the data and fits fairly well.

A b-slope of -0.9 has been determined to be applicable

to the Basin and Range (Everdon, 1970).

First Motion Plots and Cross-Section Plots

The first-motion plots are shown in Figures 13 and 14.

The first motion of each earthquake is plotted on an upper-

hemisphere stereo plot centered at the located hypocenter.

CUMULATIVE RECURRENCE CURVE
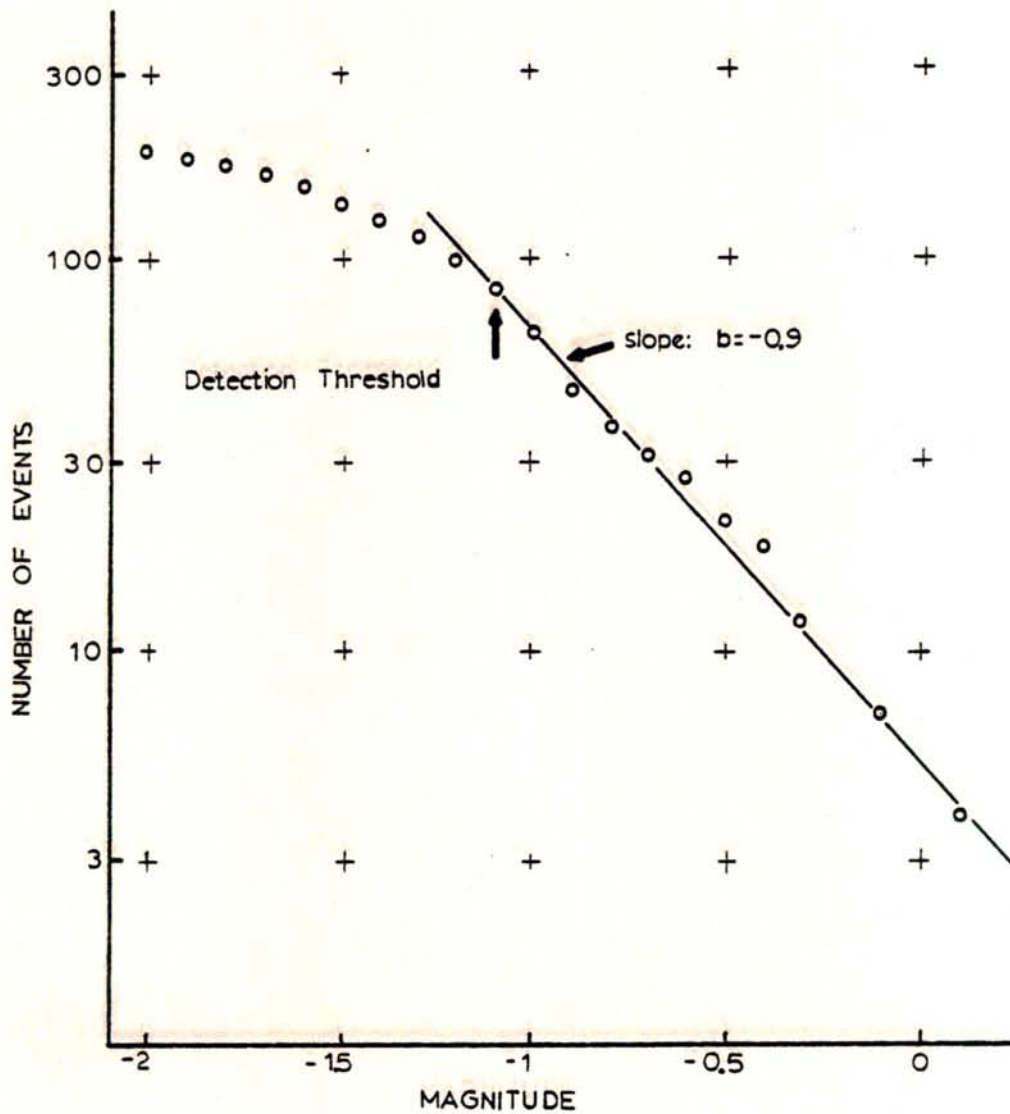
TITLE: CUMULATIVE RECURRENCE CURVE		
SCALE: N/A	APPROVED BY: PLB	DRAWN BY JRB
DATE: DEC. 16, 1976		REVISED N/A
Micro Geophysics		DRAWING NUMBER Figure 12

N

DILATATION

◄ GROUP I

306 17 56
311 6 25
310 11 59

COMPRESSION

GROUP II ►

303 16 43
306 17 35

N

COMPRESSION

DILATATION
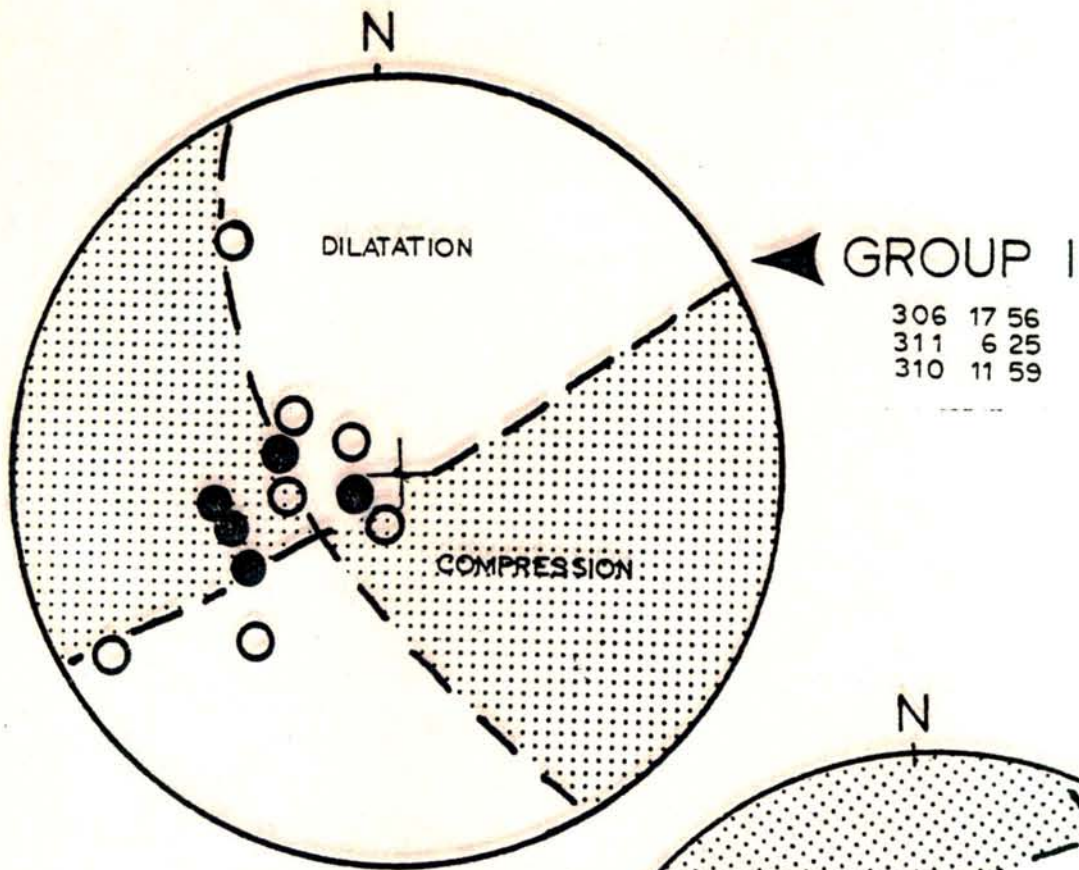
TITLE: FIRST MOTION: AREAS I & II		
SCALE: N/A	APPROVED BY: JRB	DRAWN BY PB
DATE: DEC. 18, 1976		REVISED
Micro Geophysics		DRAWING NUMBER Figure 13

Figure 14

GROUP III

292	4	45
307	7	42
310	13	30
311	18	59

GROUP IV

312 12 51

The azimuth is the earthquake-to-station azimuth and the angle measured from the vertical corresponds to the take-off angle of the ray which first reaches the station. Thus these plots are highly dependent on the velocity model assumed as both the hypocenter location (particularly the depth) will change if the velocity model is changed as will the take-off angle from the earthquake to the station.

The plots in Figures 13 and 14 will be discussed in order from north to south but the selection of actual fault-plane will be left for the interpretation section. The two most northwesterly events are located within the Stillwater Range. The first motion plots are consistent with northeast-striking normal fault planes but the strike is poorly constrained ($\pm$ 25°). The dip of these two planes is unknown.

Moving southeastward, the picture is better, but the events are also small and to one side of the network (see above signal-to-noise considerations). The three events composited together have first motion plots consistent with two planes: a N 25° W striking, deeply northeast dipping plane and a N 45° E plane with a near vertical attitude. These planes indicate either right-lateral strike-slip motion on the first plane or left-lateral strike-slip with some dip slip motion on the second. The selection of a fault plane is a matter to be interpreted, but the uncertainty in the solutions ($\pm$ 20°) should be borne in mind as the interpretation is reviewed by the reader.

The next group of earthquakes is near and in the vicinity of Station 1. First motions define two planes rather well: a roughly N-S plane with 30-40° of west dip and a northeast plane with very steep dip to the southeast. Selection of one of these planes will be difficult as the first agrees with the general trend of the epicenters but the second is subparallel with the topography and mapped faults in the area. Discussion is deferred to the section on interpretation.

The first motions due to the group of events south of the Dixie Hot Springs are composited on the last stereo plot. Due to the array geometry, these events (which were outside the prospect) have relatively few points on the first-motion plot. Two planes are shown on this plot: a N 30° W plane with 30-40° of southwest dip and a N 20° E striking plane with a steep dip to the southeast. These planes, though poorly constrained, again are consistent with either the strike of the epicenter pattern or the tectonic style of the area.

To utilize the hypocentral data, cross sections were plotted along certain azimuths of interest. Ellipses were plotted on the cross-sections to emphasize the lower accuracy of the depth figure assigned to each hypocenter. The locations of the cross sections are shown on Figure 15.

The first cross section (Figure 16) illustrates that
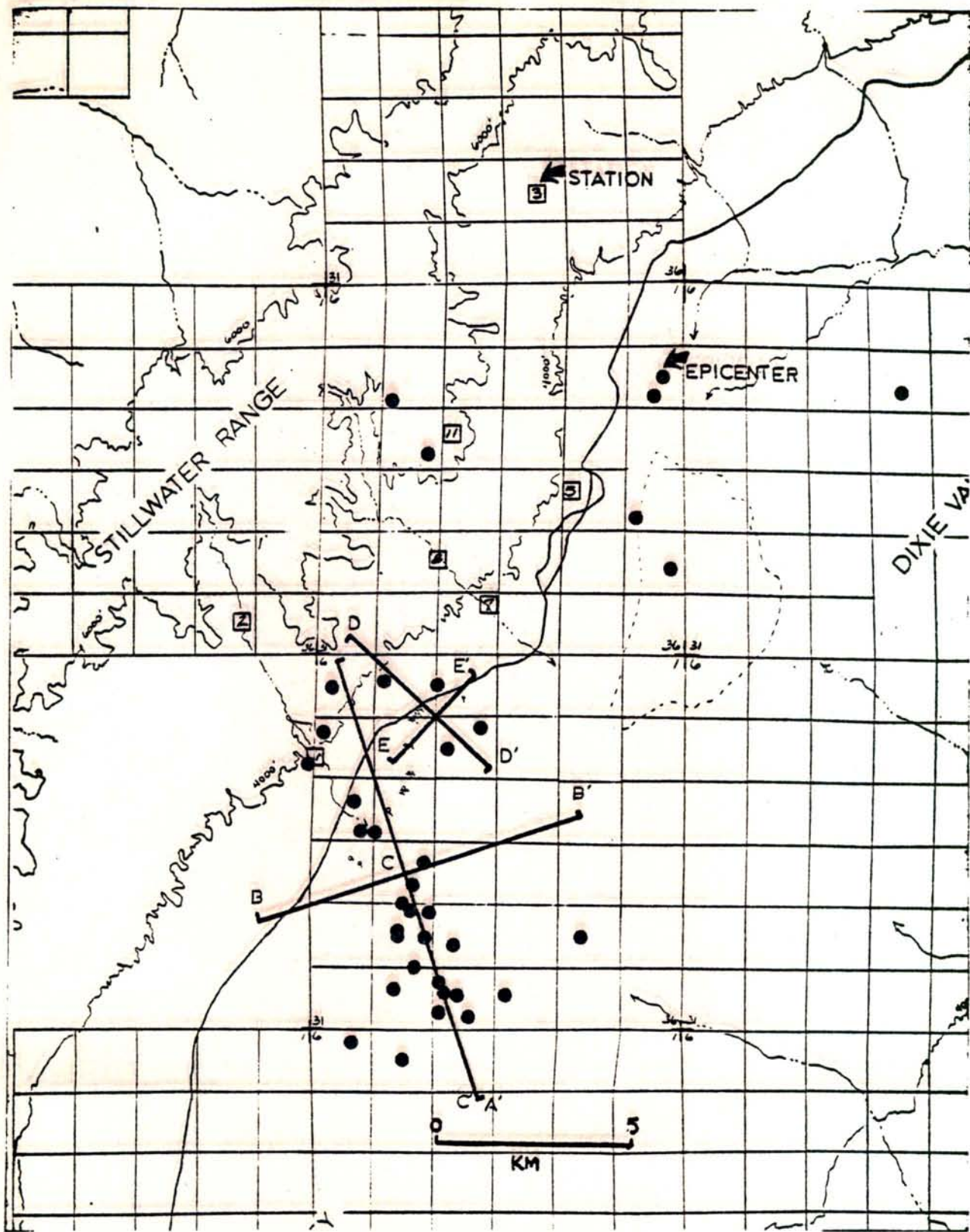
STATION

EPICENTER

N

STILLWATER RANGE

DIXIE VA.

D

E'

E

D'

B'

B

C

C' A'

0   5
KM

TITLE:	CROSSECTION LOCATION MAP	
SCALE: N/A	APPROVED BY: JRB	DRAWN BY PB
DATE: DEC 18, 1976		REVISED N/A
Micro Geophysics		DRAWING NUMBER Figure 15

N

292 4 45   309 5 33

HOT SPRINGS

307 8 17

EPICENTER

1 km.

D   DEPTH (km.) 1 2

E'

CROSSECTION

HYPOCENTER

D'
E

CROSSECTION

HYPOCENTER

DEPTH (km.) 1 2 3
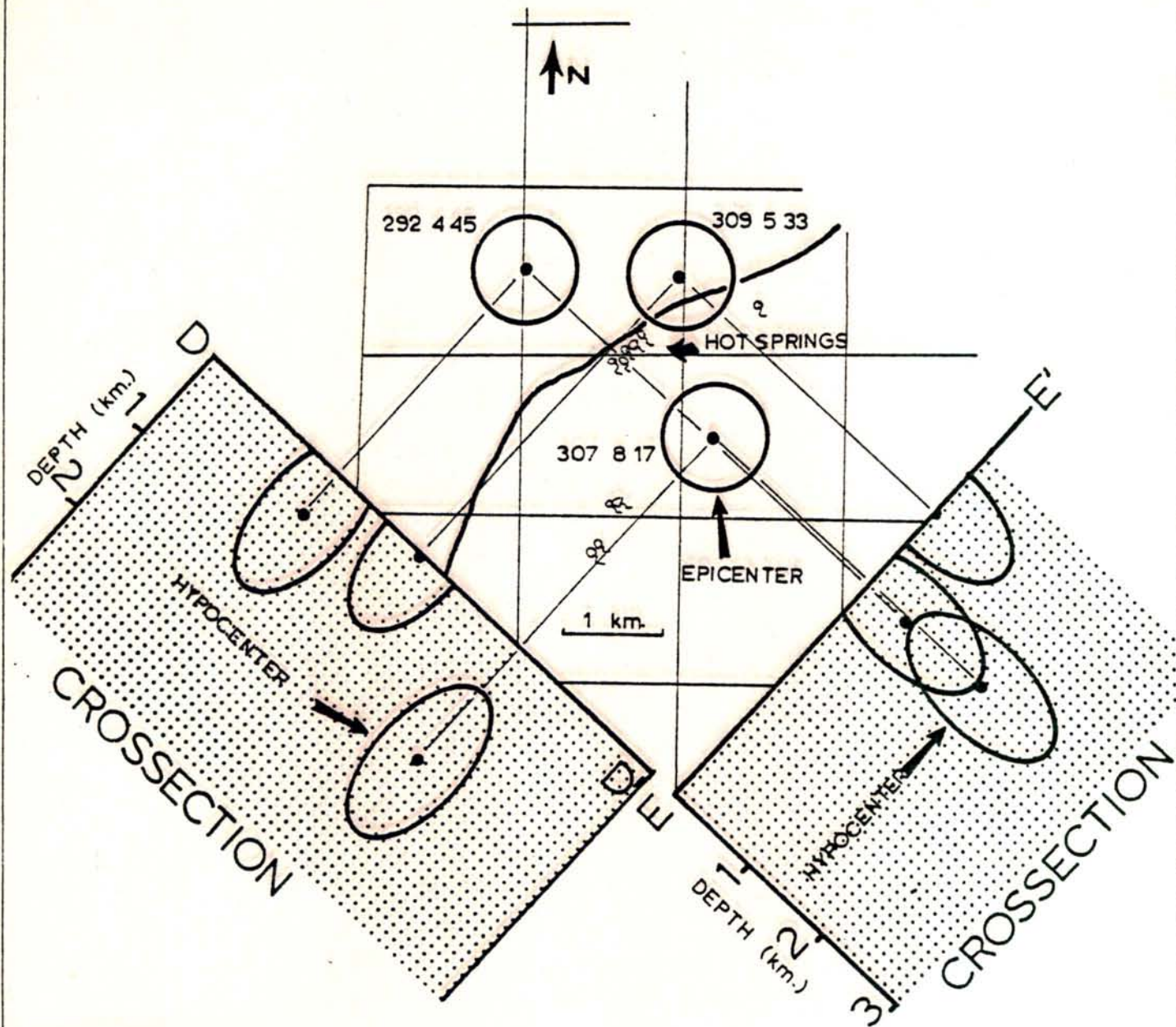
TITLE: CROSSECTIONS D-D' & E-E'		
SCALE: N/A	APPROVED BY: JRB	DRAWN BY PB
DATE: DEC. 18, 1976		REVISED
Micro Geophysics		DRAWING NUMBER Figure 16

the faulting near the north end of the hot springs is
shallow (less than 3 km). Figure 17 is an easterly view
of shallow events selected from the large group of events
to the south of the Dixie Hot Springs. These events seem
to line up on a east-north east fault-zone with about 45°
of dip to the south. The remainder of the cluster south
of the hot springs is found beneath the events on Figure 17.
These deeper events are plotted on two cross-sectional views
on Figure 18. These two cross-sectional views at right angles
indicate that the deeper events are consistent with a steeply
dipping, NW trending fault or a more moderately dipping,
NE trending fault (to within the precision of the locations).

FAULT SURFACE TRACE

T22N R35E

27

34

3

N

300 2 13

EPICENTER

PLAN VIEW

28

33

4

301 4 22

29

32

1 km

298 01 04

310 11 51

C ———————————————————— C'

DEPTH (km.)

1

2

3

4

5

6

HYPOCENTER

CROSSECTION VIEW

POSSIBLE FAULT
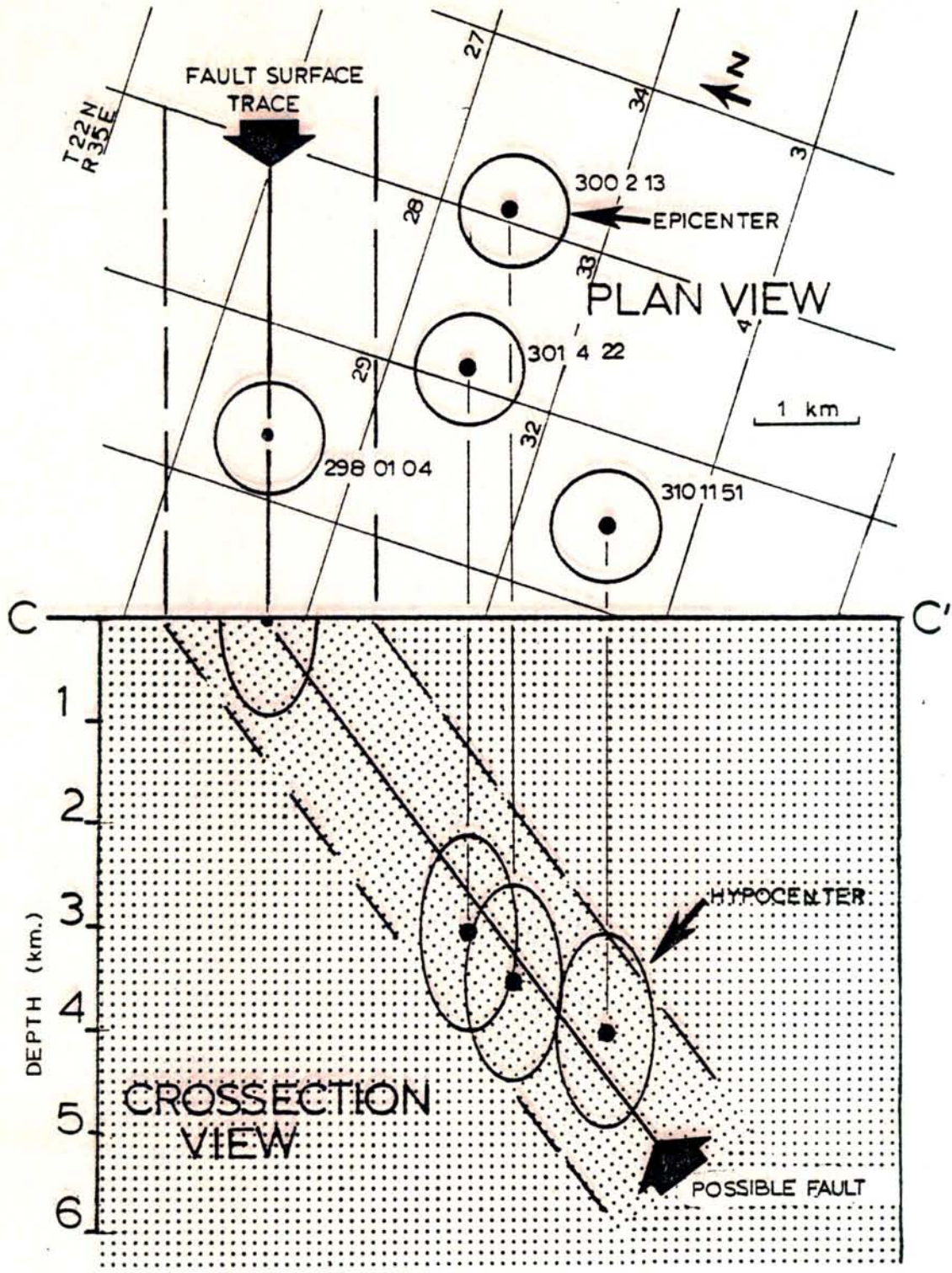
TITLE: CROSSECTION C-C'		
SCALE: N/A	APPROVED BY: JRB	DRAWN BY PB
DATE: DEC. 18, 1976		REVISED N/A
Micro Geophysics		DRAWING NUMBER Figure 17

PLAN VIEW

292 0 55
311 5 52
EPICENTER
DIXIE
HOT SPRINGS
303 8 15
308 1 16
311 20 54
310 10 15
311 18 14
311 18 59
302 15 00
301 4 52
309 4 54
307 7 42
298 10 57
310 13 30
312 12 51

1 km.

CROSSECTION VIEW

A

DEPTH (km.)
1
2
3
4
5
6
7
8
9
10

HYPOCENTER

CROSSECTION VIEW

HYPOCENTER

B
1 2 3 4 5 6 7 8 9 10
DEPTH (km.)
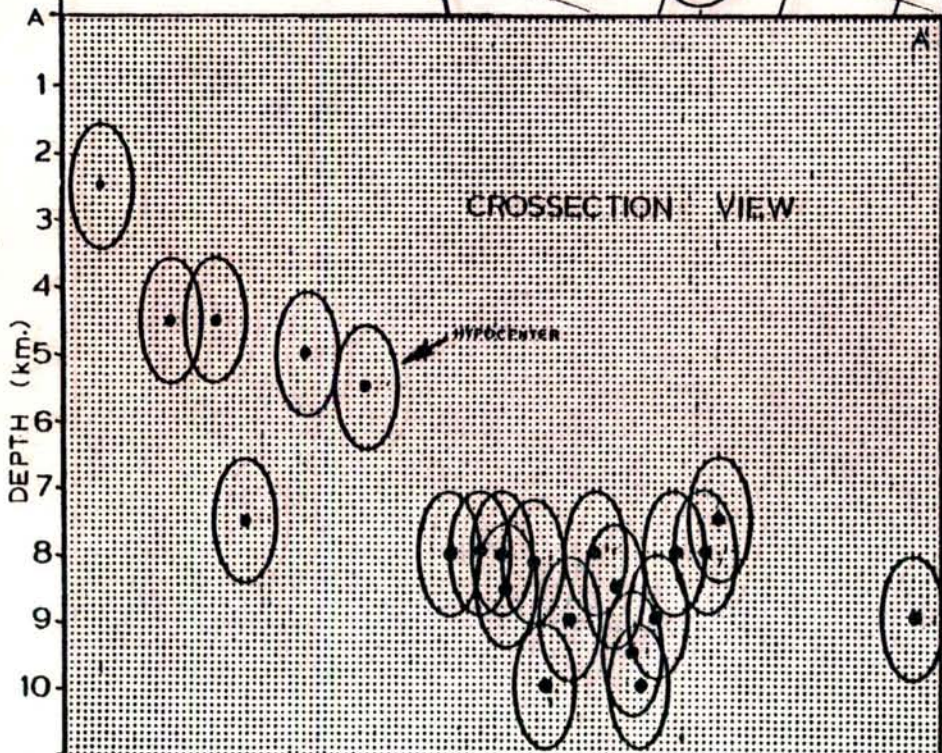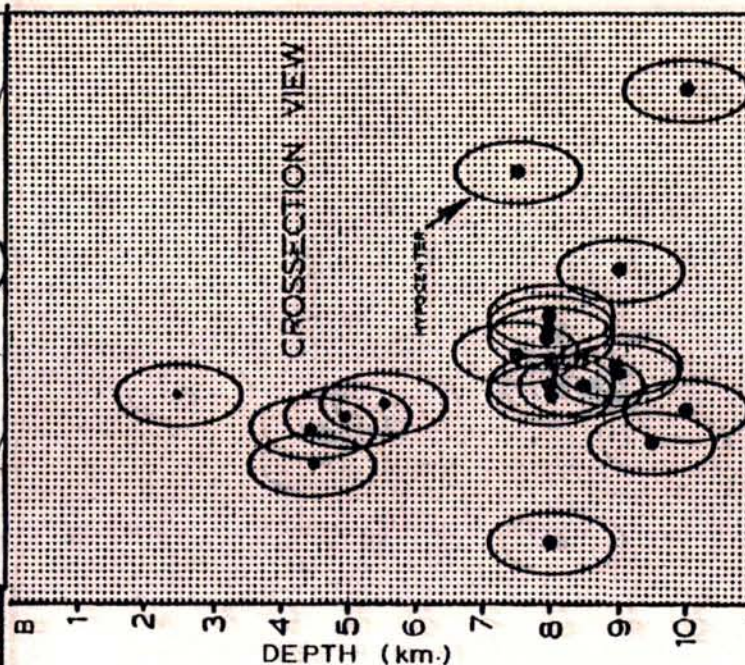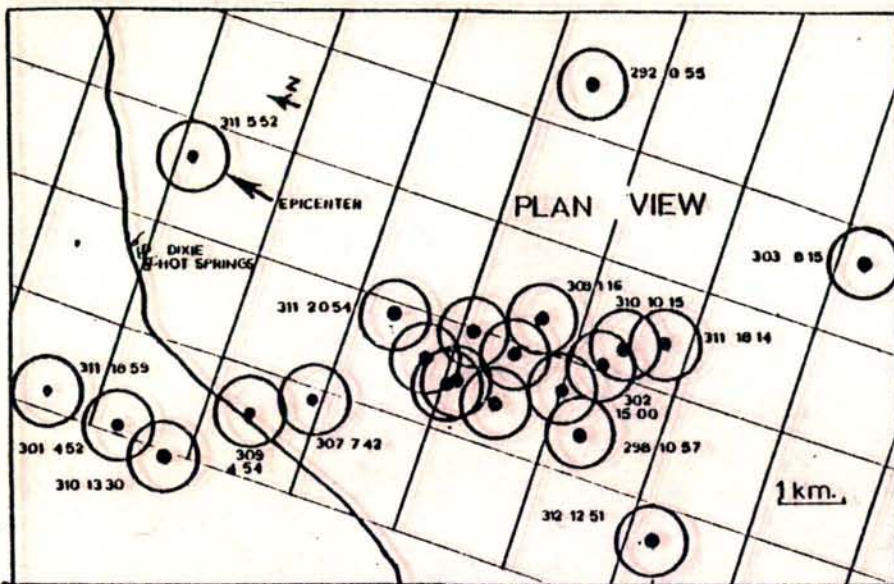
TITLE: CROSSECTIONS A-A' & B-B'		
SCALE: N/A	APPROVED BY: PB	DRAWN BY JRB
DATE: DEC. 18, 1976		REVISED N/A
Micro Geophysics		DRAWING NUMBER Figure 18

INTERPRETATION

The interpretation, as distinguished from the obser-
vations above, will focus on the prospect area. The active
seismic patterns to the south will be reviewed and then
the similar but less conclusive data on the prospect will
be interpreted from the viewpoint of homogeneity of tectonic
style from south to north. Due to the historical macroseismic
activity in the area, care must be exercised in equating
seismicity with geothermal activity. The fault-plane solu-
tions, due to the ambiguity problem, have no unique inter-
pretation. The favored interpretation of the seismicity is,
however, consistent with the geological patterns observed
both south and north of the prospect area.

The historical seismicity (Figure 3) indicates an aseismic
gap in the prospect area. The fault model of Ryall and Malone
(1971) (Figure 4) indicates long oblique-slip NNW-trending
segments (with significant strike-slip components) connected
by short NE-trending dip-slip segments. The preferred
interpretation of the cluster of events south of the hot
springs is that they are part of one of the NW-trending
oblique slip zones. Near where this zone intersects the
highway, the events are interpreted to lie on a NE-trending
dip-slip zone. This zone trends into the prospect area and

is intersected by another oblique-slip zone which has a NNW-trend.

A persuasive point for this interpretation is the fact that the NE trending normal fault zone is subparallel and spatially close to the geologically mapped boundary fault of the Stillwater range.

Two events high up in the Stillwater range are almost certainly on a NE-trending dip-slip zone that is down towards the valley.

An alternative interpretation of all seismicity recorded off the prospect is NE-trending en echelon normal faults down to the valley. However on the prospect the fault-plane solution requires and constrains a strike-slip mechanism. The mechanisms are either a right-lateral, N 20° W striking, fault or a left-lateral, NE-striking fault. The important conclusions is that in or near the prospect the mechanism of faulting changes and fault intersections are present in the prospect area.

The group of events south of the hot springs is in a historical swarm zone. A swarm is defined as a large number of events concurrent in space and time. The events recorded during this survey are consistent with this background. To illustrate this observation, a qualitative strain-release map was prepared as Figure 19. Events to the north are enclosed by a dotted contour as all events detected are present on this map. The southern group
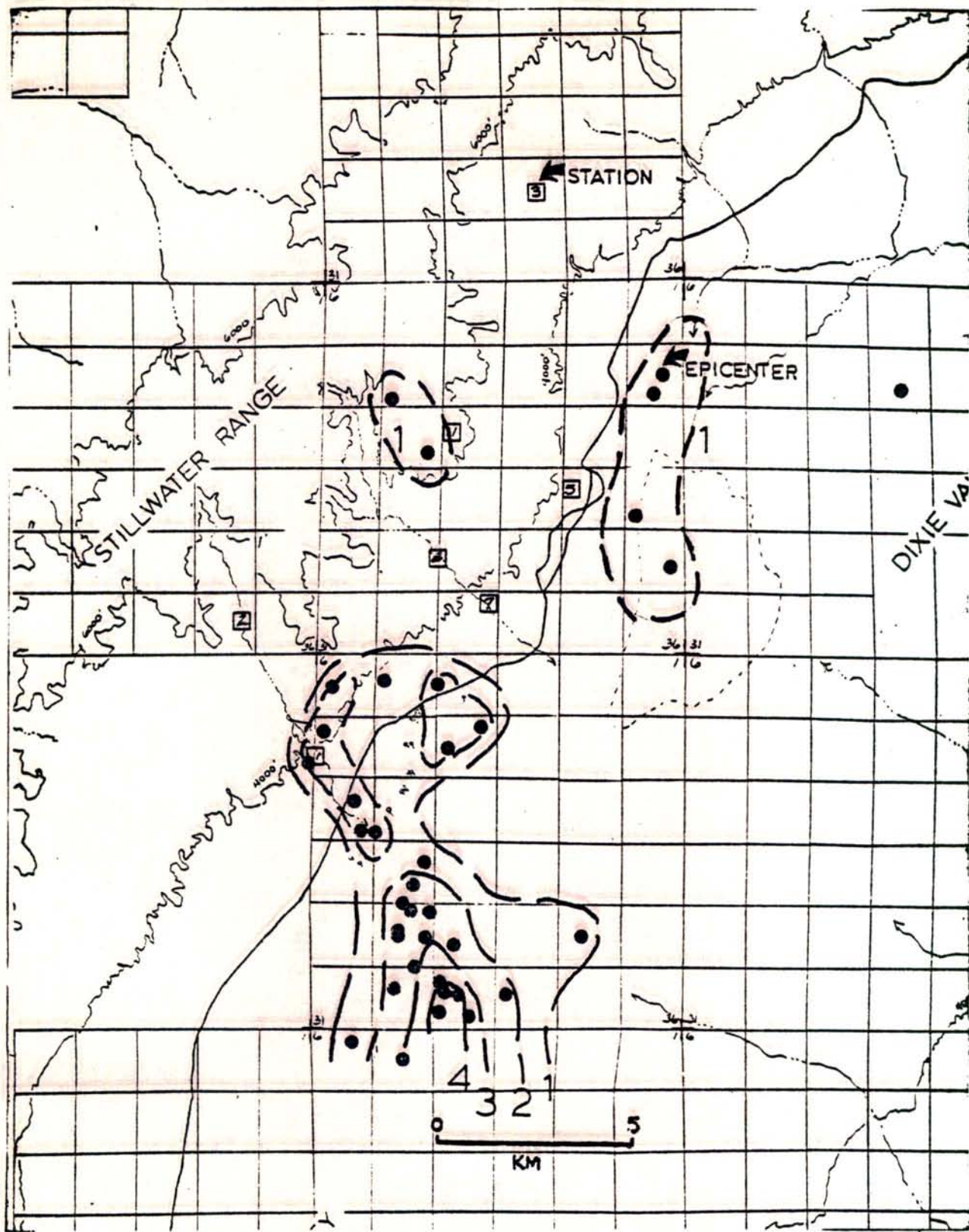
Contour values represent relative strain release.

| TITLE: QUALITATIVE STRAIN RELEASE		
SCALE: N/A	APPROVED BY: JRB	DRAWN BY PB
DATE: DEC 18, 1976		REVISED N/A
Micro Geophysics		DRAWING NUMBER Figure 19

has numerous contours as many small events were detected in the swarm zone south of the hot springs. Figure 20 is a schematic diagram delineating the nature of the regional tectonics from south to north. The northeast striking faults in Figure 20 are interpreted to be oblique slip, the northwest striking fault, dip-slip. Figure 21 indicates the volume of seismicity near station 2. Note that the scale is logarithmic; the majority of these events are 10-12 km from station 2, i.e. south of the Dixie Hot Springs.

The seismicity rate in the immediate vicinity of the prospect is not high, near one event per 3-5 days. However, with respect to seismic risk, the important point is the extension of the tectonic style from the Fairview Peak-Dixie Valley part of the Nevada Seismic zone northward past the prospect. Such an extension has been previously proposed on geologic grounds, but the microearthquake evidence from this survey definitely indicates that such an extension is likely. The implications of this extension are in the area of seismic risk to wells or other structures built on this zone. A pessimistic view would be that events as large as the Fairview Peak-Dixie Valley earthquake (Richter magnitude 6.8!) could happen within the prospect area. Careful economic analysis, return-time estimates, and ground-acceleration maps should be prepared if commercial development of the geo-thermal resources is contemplated.

This interpretation has indicated the likelihood of active fault intersections within the prospect area, a moderate but important seismicity rate, and an extension of the regional tectonics of a major seismic zone south of the prospect area.

STATION

EPICENTER

STILLWATER RANGE

DIXIE VA

D

U

D

D

DIP

U

D

N

0   5

KM
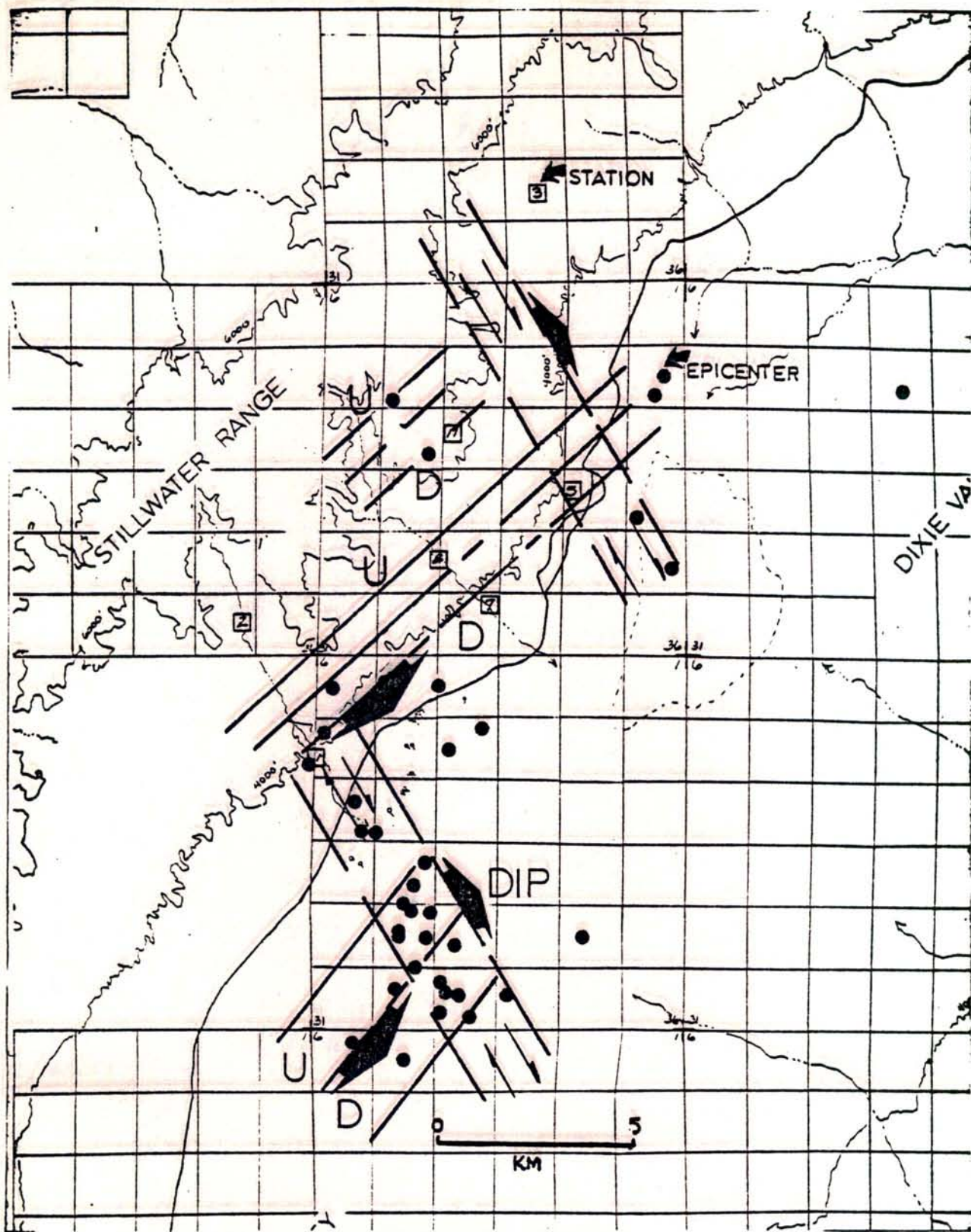
TITLE: REGIONAL TECTONICS		
SCALE: N/A	APPROVED BY: JRB	DRAWN BY PB
DATE: DEC 18, 1976		REVISED N/A
Micro Geophysics		DRAWING NUMBER Figure 20
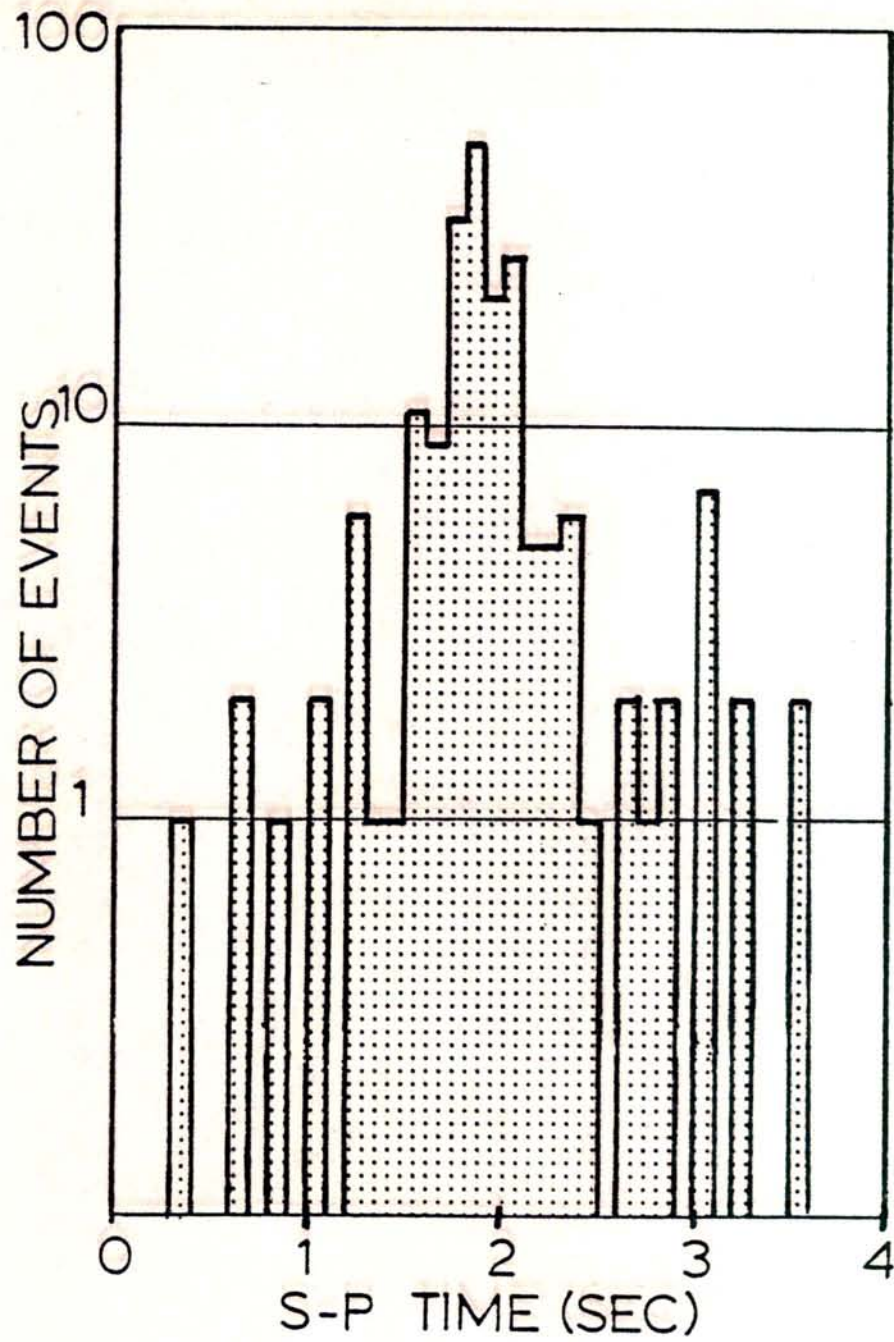
TITLE: S-P TIME FROM STATION 2		
SCALE: DEC. 18,1976	APPROVED BY: JRB	DRAWN BY PB
DATE: N/A		REVISED N/A
Micro Geophysics		DRAWING NUMBER Figure 21

CONCLUSIONS

1. Seismically active faults are present in the prospect
   area. First-motion studies indicate fault inter-
   sections that are seismically favorable areas for the
   occurrence of earth steam are present near station 5
   on the prospect area.

2. Upon confirmation of a heat source and a favorable
   groundwater regime, the prospect should be tested for
   commercial production of geothermal resources.

3. The seismic risk in this area is high. This survey
   confirms the extension of the Nevada Seismic Zone across the
   prospect area.

RECOMMENDATIONS

1. The existence of a heat source and a favorable water
    supply situation should be confirmed by electrical
    resistivity and hydrologic studies.

2. Upon confirmation of a favorable geologic environment
    and from the seismological point of view, this area is
    an excellent geothermal prospect.

3. When commercial exploitation is begun, seismic activity
    associated with the withdrawal and injection of fluids
    must be carefully monitored in order to isolate any
    adverse environmental effects.

4. This area is subject to substantial seismic risk.
    Construction in the area must conform to adequate build-
    ing codes in order to minimize the probable earthquake
    risk.

Micro Geophysics

REFERENCES

Brune, James and Clarence Allen, 1967, A microearthquake survey
of the San Andreas fault system in Southern California,
BSSA, vol. 57, no. 2, p. 277.

Chinnery, Michael A., 1969, Earthquake Magnitude and Source
Parameters, BSSA, vol. 59, no. 5, p. 1969.

Douglas, B. M. and Ryall, A., 1972, Spectral Characteristics
and stress drop for microearthquakes near Fairview Peak,
Nevada, JGR, vol. 77, no. 2, p. 351.

Evernden, J. F., 1970, Study of Regional Seismicity and Asso-
ciated Problems, BSSA, vol. 60, no. 2, p. 393.

Gumper, F. J., and Scholz, C., 1971 Microseismicity and
tectonics of the Nevada seismic zone, BSSA, vol. 61,
no. 5, p. 1413.

Hamilton, R. M. and L. J. P. Muffler, 1972, Microearthquakes
at the Geysers Geothermal area, California, JGR, vol. 77,
no. 11, p. 2081.

Herring, A. T., 1967, Seismic refraction study of a fault zone
in Dixie Valley, Nevada, A. F. Cambridge Research Labs
Final Scientific Report Part II, AFCRL - 66-848.

Lange, A. L. and W. H. Westphal, 1969, Microearthquakes near
the Geysers, Sonoma County, California, JGR, vol. 74, p. 4377.

Meisler, L. J., 1967, Seismic refraction study of Dixie Valley,
Nevada, A. F. Cambridge Research Labs Final Scientific
Report Part I, AFCRL-66-848.

Meister, L. J., Buford, R. O., Thomson, G. A. and R. C. Kovach,
1968, Surface-strain changes and strain energy release
in the Dixie Valley-Fairview Peak area, Nevada, JGR,
vol. 73, no. 18, p. 5981.

Peters, David and Robert Crosson, 1972, Application of pre-
diction analysis to hypocenter determination using a
local array, BSSA, vol. 62, no. 3., p. 775.

Romney, C., 1957, Seismic waves from the Dixie Valley-Fairview
Peak earthquakes, BSSA, vol. 47, no. 4, p. 301.

Ryall, A., 1970, 1971, <u>Bulletin of the Seismological Laboratory,</u> Mackay School of Mines.

Ryall, A. and Mallone, S. D., 1971, Earthquake distribution and mechanism of faulting in the Rainbow Mountain-Dixie Valley-Fairview Peak area, central Nevada, <u>JGR,</u> vol. 46, no. 29, p. 7241.

Slemmons, D. B., 1957, The Dixie Valley-Fairview Peak, Nevada, earthquakes of December 16, 1954: geologic effects, <u>BSSA,</u> vol. 47, no. 4, p. 353.

Stauder, W. and Ryall, A., 1967, Spatial distribution and source mechanism of earthquakes in central Nevada, <u>BSSA,</u> vol. 57, no. 6, p. 1317.

Ward, P. L., 1972, Microearthquakes: Prospecting tool and possible hazard in the development of Geothermal Resources, <u>Geothermics,</u> vol. 1, no. 1, p. 3.

Ward, P. L. and S. Bjornson, 1971, Microearthquakes, Swarms and Geothermal areas of Iceland, <u>JGR,</u> vol. 76, no. 17, p. 3953.

Ward, P. L. and R. H. Jacob, 1971, Microearthquakes: In the 'Anuachapan Geothermal Field, El Salvador Central America, <u>Science,</u> vol. 173, p. 328.

Westphal, W. H. and Lange, A. L., 1967, Local seismic monitoring Fairview Peak area, Nevada, <u>BSSA,</u> vol. 57, no. 6, p. 1279.

APPENDIX

INSTRUMENTATION

The microearthquake network, used for geothermal exploration and deployed by MicroGeophysics Corporation, consists of from six to eight independent microearthquake recording systems. Each system contains an L-4-C vertical seismometer, a MEQ-800-B visual drum recorder with an integral timing system synchronized to universal coordinated time (U.T.C.). Figure 1 is a schematic of the microearthquake recording system. A detailed explanation of the component parts is given below.
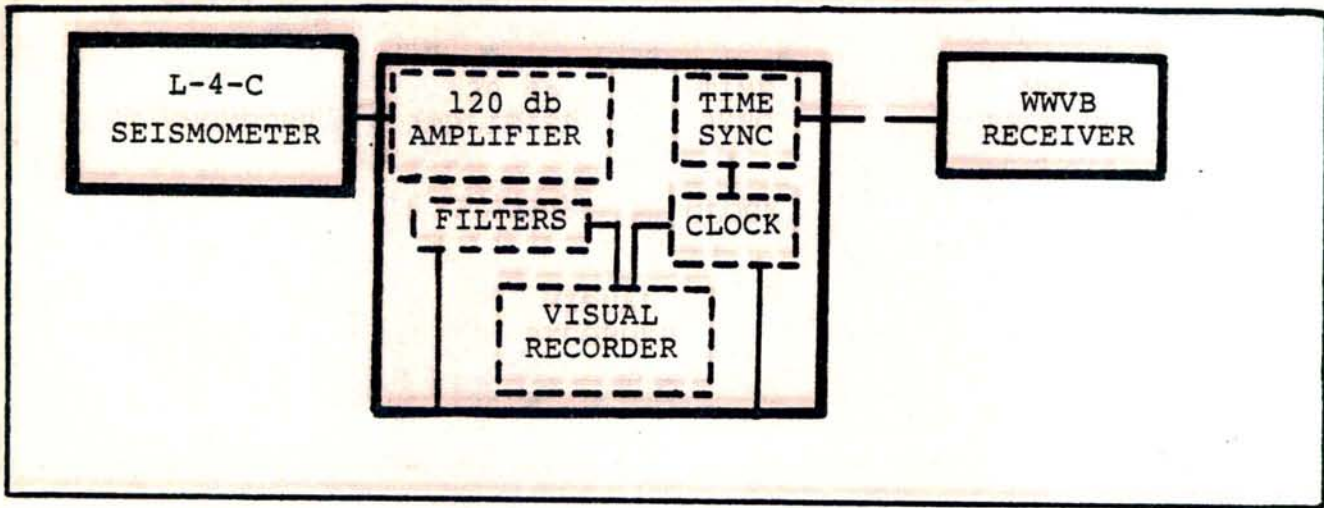

Figure 1

<u>L-4-C</u>

The L-4-C is a one-hertz-natural-frequency vertical seismometer. The damping is 0.6 of critical damping. The L-4-C has an output of 6.9 volts per inch/second.

Geophones are planted on solid rock in protected locations consistent with the geometrical requirements of appropriate array shape and access considerations. The field monitor allows a rapid evaluation

of each geophone plant over a 24 hour period and poor stations (noisy, bad earthquake signatures, low gain) are immediately moved to favorable sites.
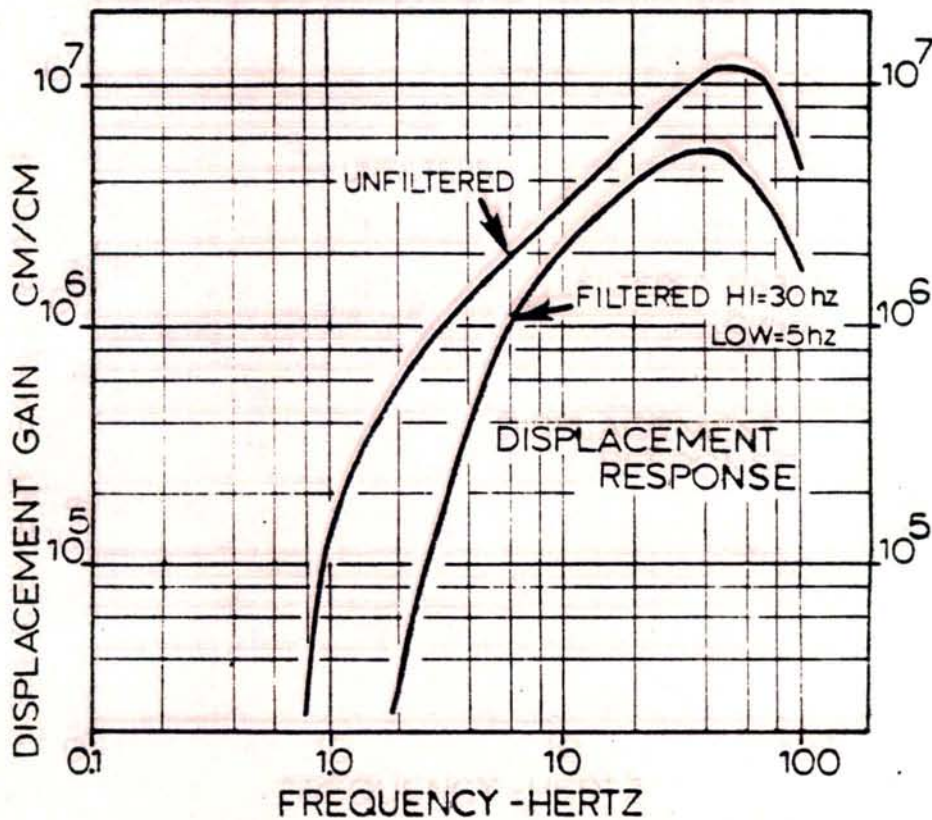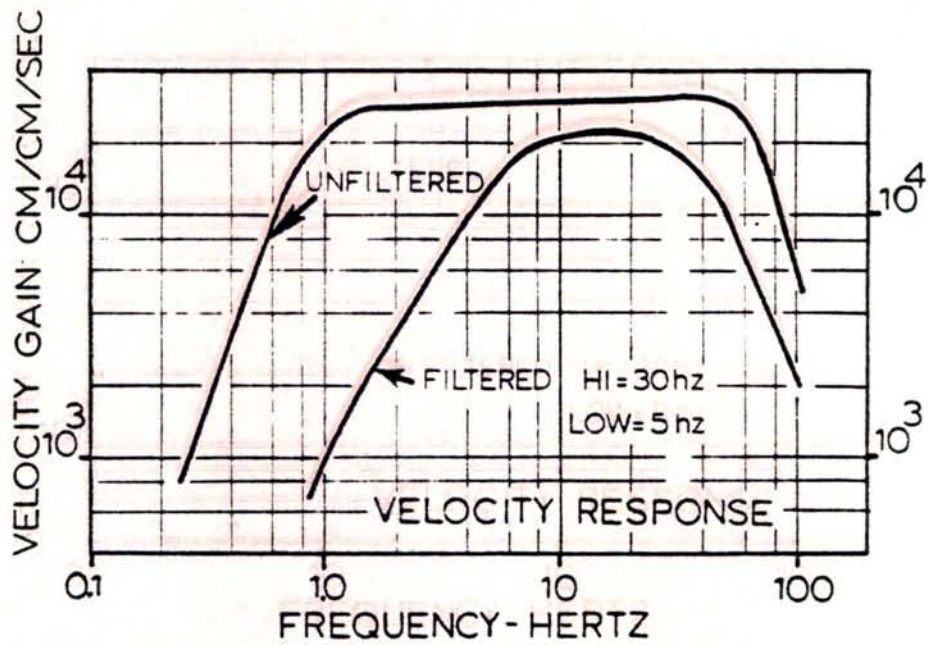
MEQ-800-B

The MEQ-800-B is a visual microearthquake recorder. The smoked drum recording has a nominal 120mm/min rotation speed with 1mm spacing between succeeding traces. The stylus and trace width is 0.05mm. The amplifier has a maximum of 120db of gain and selectable high and low cut filters. The low cut filter has selectable corners at 1, 5 and 10 Hz. The high cut filter has selectable corners at 10, 20, and 75 Hz. The amplifier gains can be changed by precise 6db steps down from 120db. The maximum pen deflection is $\pm$25mm and can be limited under severe ground noise conditions to $\pm$10mm or $\pm$5mm.

The integral timing system consists of a clock, whose drift rate is less than $\pm$1 part in 10^7 (approximately $\pm$10ms per day) and can be set to standard time and adjusted at 16ms increments. Time is displayed on each trace by a slight deflection of the pen each second.

The frequency characteristics of the instrument are summarized in Figure 2I. Both the velocity and displacement response for the MEQ-800-B microearthquake system are shown. The displacement response at a particular frequency (f) can be calculated by multiplying the velocity gain at f times 2 f. The filter response and gain level shown are typical settings for operations in the western continental United States.

INSTRUMENT RESPONSE

The velocity and displacement response of the MEQ-800-B are plotted at the gain setting of +96db

WWVB

WWVB is the radio call code for the National Bureau Standards 60khz time-standard station in Fort Collins, Colorado. The WWVB time standard is used to set and synchronize the microearthquake system clocks. As shown in Figure 3A below, the signal consists of 60 markers each 1 minute, with one marker each second. (Time progresses from left to right) each marker is generated by reducing the power of the carrier by 10db at the beginning of the corresponding second and restoring it:

1) 0.2 seconds later for a binary zero

2) 0.5 seconds later for a binary one

3) 0.8 seconds later for a 10 second position marker for a minute reference marker.

Point A is 258 Days, 18 hours, 42 minutes and 36 seconds.
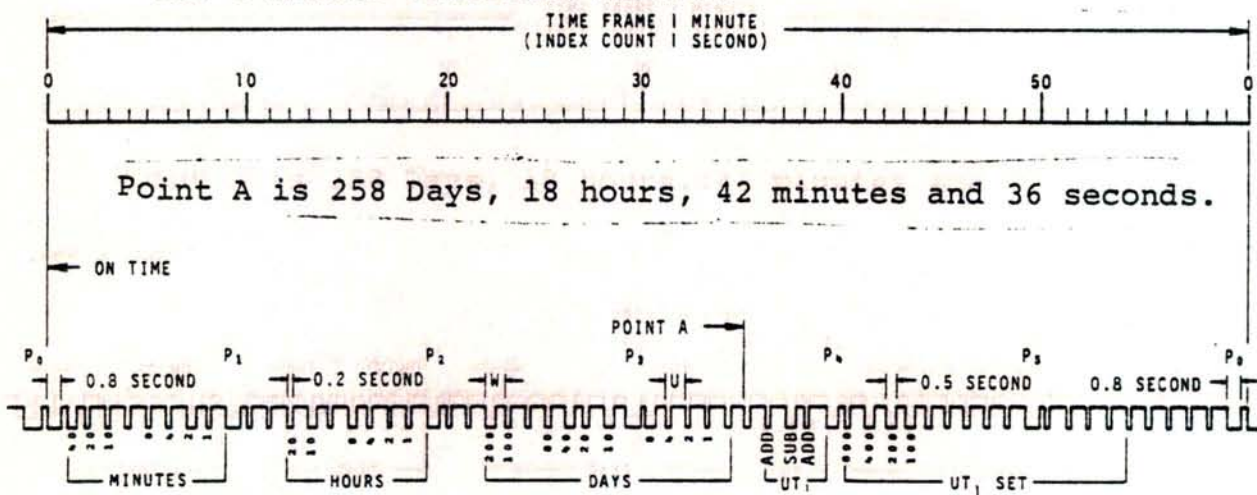
Figure 3

The WWVB code (as shown in Figure 3) is recorded daily on the visual drum as absolute time and date identification of the record, and is used to synchronize each MEQ system to standard time.

The MEQ systems clocks are synchronized daily with WWVB by comparing (on an oscilloscope) the beginning of the WWVB second pulse with the MEQ-800-B internally generated one-second pulse. This comparison can be done to ±2 milliseconds. Daily records are kept

on the amount of correction for each clock. These time corrections
are then applied to the records. Common corrections are on the order
of 15ms per day or less than one millisecond per hour.

DATA

An example of the output of a microearthquake system is shown in
Figure 4.

The smoked paper record is used at the time of the recording (in
the field) to estimate the seismicity and to locate any recorded
microearthquake approximately. The smoked paper records can be picked
under magnification to a precision of less than $\pm$30ms. A level of
$\pm$30ms timing precision is sufficient to insure that the location
uncertainty is almost entirely governed by the inaccuracies in the
velocity model (Johnson, 1975).

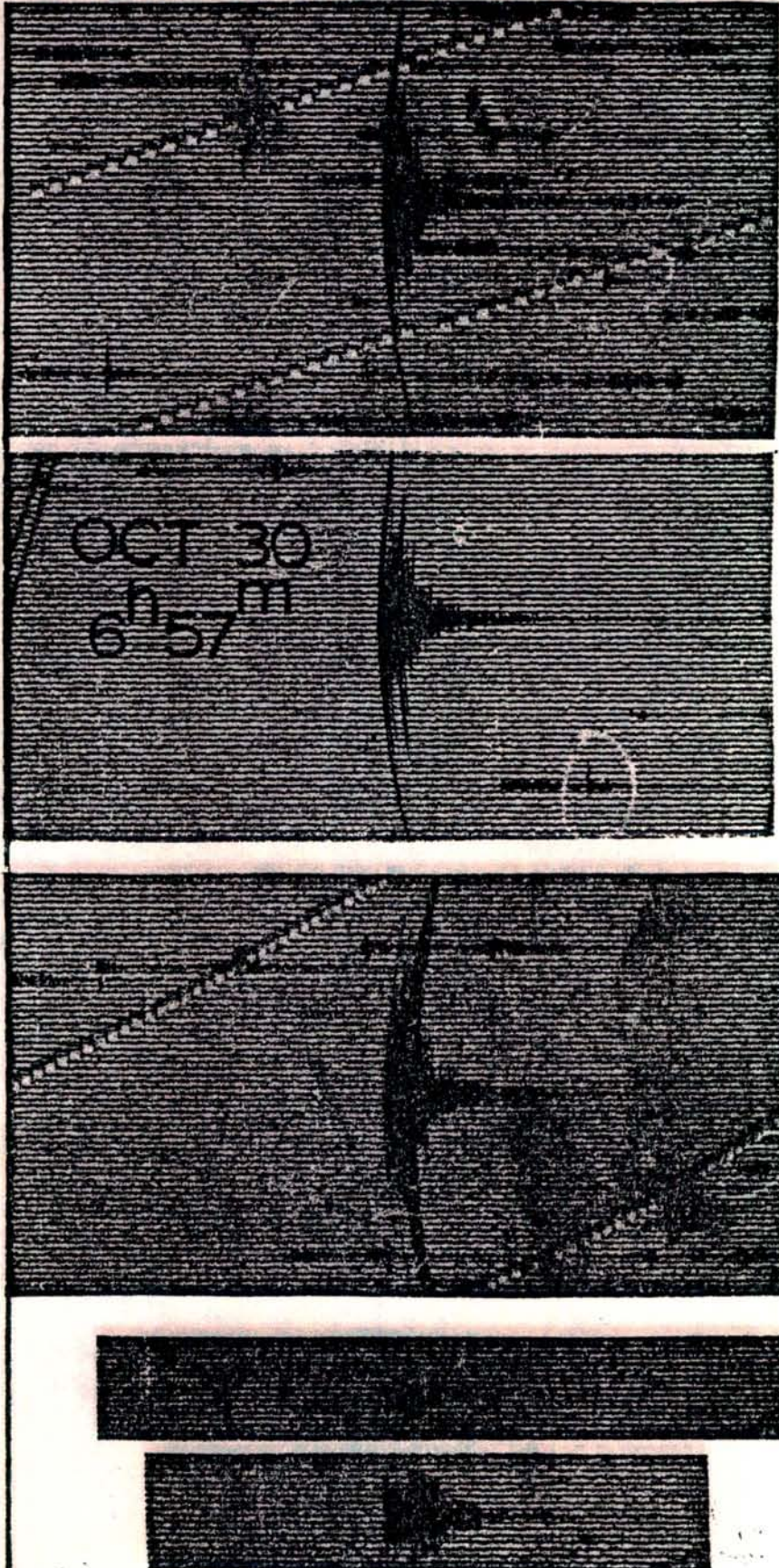# EXAMPLE OF A LOCAL EVENT

GAIN X 1000

STATION NUMBER

560

2

OCT 30
6ʰ57ᵐ

560

3

560

9

35

7

1130

8

1 MIN

fig 4

Epicenter Appendix

Located Events

Day	Time	X (km)	Y (km)	Z (km)	M
292	445	14.8	34.0	.5	−0.9
293	055	20.5	27.5	10.0	0.1
293	934	16.0	26.6	8.0	−0.8
293	1059	15.5	28.4	8.5	−0.6
293	1615	15.8	28.3	8.0	−0.6
298	104	15.6	27.5	0.0	−0.8
298	1057	15.5	26.2	9.5	−0.5
300	213	18.0	26.0	3.5	−1.9
301	422	16.5	26.0	3.0	−1.0
301	452	13.3	32.6	4.5	−2.2
301	1810	16.5	12.3	1.5	0.1
302	348	−5.8	55.2	22.5	−1.3
302	1500	16.7	26.2	9.0	−0.3
303	815	19.0	22.8	9.0	−1.0
303	1643	15.1	41.3	4.0	−2.0
306	320	4.8	21.2	0	3
306	412	16.0	28.7	8.0	−1.0
306	1735	16.2	39.9	1.0	−1.4
306	1756	22.2	41.3	1.0	−0.4
307	742	14.7	30.0	5.5	−1.0
307	817	16.8	32.3	1.5	−1.1

Epicenter Appendix - Located Events

- 2 -

Day	Time	X (km)	Y (km)	Z (km)	M
308	1955	14.8	30.2	4.0	-1.3
309	116	16.8	27.1	8.0	-0.5
309	454	14	30.9	5.0	-1.6
309	533	16.5	33.9	0	-1.3
309	1657	-9.2	38.7	4.5	-0.3
310	931	16.3	28.2	8.0	0.2
310	1015	16.9	26.0	8.0	-1.0
310	1028	16.5	25.6	8.0	-0.4
310	1151	15.5	24.2	4.0	-1.0
310	1159	22.6	36.8	8.0	-0.9
310	1330	13.0	31.9	4.5	-1.1
311	552	18.7	33.0	7.5	-0.6
311	625	21.5	38.2	8.0	-1.4
311	1814	17.0	25.3	7.5	-0.6
311	1859	13.4	33.8	2.5	-1.0
311	2047	16.2	27.5	9.0	-0.3
311	2054	16.2	29.5	8.0	-0.1
312	1251	14.2	24.7	8.0	-0.1
313	240	15.3	27.5	10.0	-1.6
313	807	22.7	42.0	4.5	-1.8
313	808	29.1	41.7	5.0	-2.9

Micro Geophysics

Epicenter Appendix - Located Events

- 3 -

Day	Time	X (km)	Y (km)	Z (km)	M
313	838	13.4	18.7	0	1.0
313	1115	21.9	52.2	7	0.3

The origin is located at latitude $39^\circ 30'$ N, longitude $118^\circ 15'$ W. Z is the event depth below a datum of 1 km above sea level. Positive X and Y are east and north respectively. M is event magnitude.
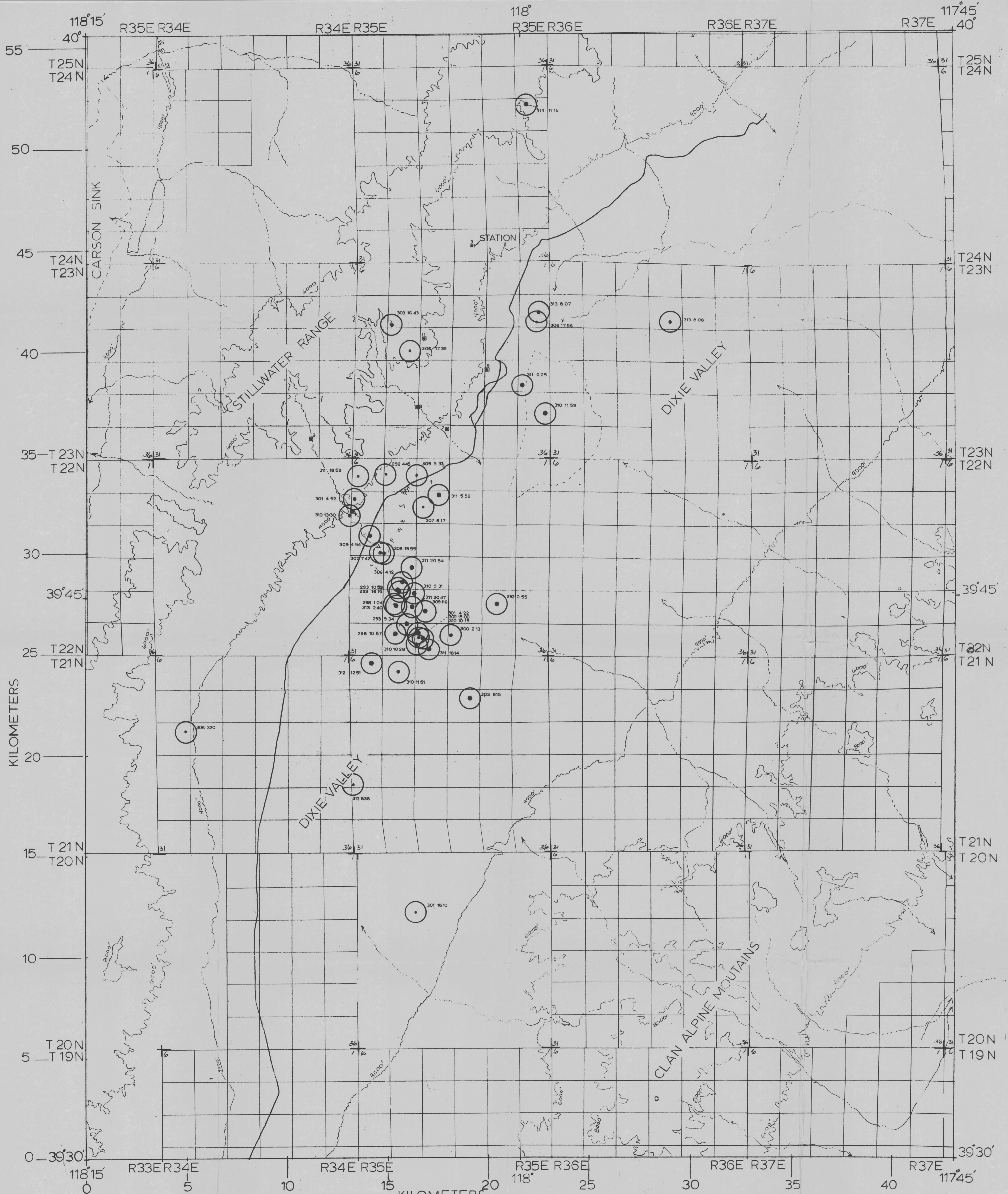
MICROGEOPHYSICS
DIXIE VALLEY
NOV '1976